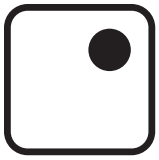

ACTA·GRAPHICA

JOURNAL FOR PRINTING SCIENCE AND GRAPHIC COMMUNICATIONS

UDC 655(05) • CODEN: AGGRER • ISSN 0353-4707

2/16

ACTA GRAPHICA 27 (2016) 2, 1–70

A Word from the Editors-in-chief

Dear Readers,

in front of you is new double issue of Acta Graphica in which, we believe, you will find interesting articles in the scientific areas of your interest.

"It's not the strongest of the species that survives, nor the most intelligent; but the one most responsive to changes."

Editors-in-Chief

Damir Modrić

Miroslav Mikota

Contents

Color Appearance of the Neon Color Spreading Effect

Damir Vusić, Robert Geček, Krunoslav Hajdek

Dept. of Multimedia, Design and Application, University North, Varazdin, Croatia

Abstract

As a part of this paper, the influence of various parameters within the target process of graphic reproduction on the color appearance of the neon color spreading effect was investigated. The shift in a color appearance qualitatively is determined through the calculation of changes in perceptual attributes of color, i.e. differences in lightness, chroma and hue.

The influence of different media (printed images, and LCD display) in the "cross-media" system was examined, as well as the role of the inserted segment color choice and background of the primary stimulus as an element of design solutions. These parameters were evaluated in a variety of ambient conditions and under the observation of three CIE standard light sources and illuminants.

It was found that it was mostly the changes of the chroma and lightness. The change in the color hue is the lowest.

Keywords: Color appearance, graphic reproduction, neon color spreading, perceptual attributes of color

1 Introduction

Presentation of color uses different media (printed images, LCD displays, TVs, cellphones, projectors etc.) to present to the viewer a "cross-media" reproduction system. Ensuring that the conditions for identical color perception, regardless of the medium of communication and regardless of all other parameters that influence the perception of color, is the basic function of such a system [1, 2]. Graphic color reproduction via a variety of media using different methods and procedures always leads to a change to the form of color data. The diversity of visual color perception creates the need for colorimetric research and the building of a psychophysical model of the human experience of color.

Color appearance under certain viewing conditions can be described via tristimulus color data. These include tristimulus functions represented by three parts of light spectrum. They define the color unambiguously: two colors with the same tristimulus functions, under the same observation conditions, can be seen as equal by a standard observer (and vice versa). This is information about the psychophysical properties of light leaving the surface of an object - color hue, color chroma and color lightness [3]. These characteristics are the perceptual attributes of color.

The perception of color can be described as the ability to recognize the difference between wavelengths of light. The perception of color at the end point is not the result of seeing the wavelength or the light but rather the experience of the illuminated object [4, 5].

Achieving uniformity of color (i.e. the correct color appearance) within a "cross-media" system is questionable under conditions which include occurrence of various psychophysical visual effects [6, 7, 8, 9].

There are a significant number of psychophysical visual effects the manifestation of which have yet to be fully explored. One of these is the neon color spreading effect. The effect of this is the shift in color appearance by creating an

illusory extension of primary stimulus colors in the background of a given graphic reproductions in the grid area of the same size as the inserted segment of the primary stimulus, but also in the process of shaping templates as part of the development of a design solution [10]. Existing research into the the neon color spreading effect within the "cross-media" system of graphic reproduction has determined the intensity of the effect within certain parameters [10, 11, 12].

Determining the color appearance in a graphic reproduction process, in conditions with manifested psychophysical visual effects, is based on assessment of a psychophysical experience of an individual perceptual attributes of color (hue, lightness and chroma). This is possible by application of colorimetric and psychophysical research methods. Combined, they create a methodology for determining the physical values of visual perception of a color stimulus.

The aim of this study is to determine the impact of various parameters within a graphic reproduction system on the color appearance of the neon color spreading effect. Shift in a color appearance is an error in color perception. A qualitative analysis of the shift in a color appearance shows that the perceptual attribute of color is likely to change the most.

2 Experimental Part

2.1 Research Description

The colorimetric part of the research was conducted using a "Gretagmacbeth Eye-One" reflective spectrophotometer. Formed reference fields in a printed color chart were attributed by the corresponding CIE *L*a*b** values. Based on this data, values between color differences ΔE^*_{94} in each field were calculated with respect to the colorimetric values of the printing substrate [13].

A psychophysical evaluation (a visual evaluation of test samples) was carried out using simultaneous binocular techniques to harmonize the relationship between the original and the reproduction (the reference and the test sample) in the "cross-media" system [14].

The research was conducted using a sample of 30 observers (16 male and 14 female observers with an average age of 21).

A stationary box for the observation of the test samples, "the Judge II-S" was used.

The color appearance shift caused by the manifestation of neon color spreading effect is obtained by calculating the perceptual attributes of color: lightness difference (ΔL^*), chroma difference (ΔC^*_{ab}) and hue difference (ΔH^*_{ab}). The reference values used are the CIE $L^*a^*b^*$ of the same size as the background. Dominant or pronounced changes in specific perceived perceptual attributes of color describes the color appearance shift of the manifested effect.

Changes of the perceptual attributes of color are calculated using the following equations [13]:

$$\Delta L^* = L^* - L^*_{ref} \tag{1}$$

$$\Delta C^*_{ab} = C^*_{ab} - C^*_{abref} \tag{2}$$

$$\Delta H^*_{ab} = \sqrt{\left[\left(\Delta a^*\right)^2 + \left(\Delta b^*\right)^2 - \left(\Delta C^*_{ab}\right)^2\right]} \tag{3}$$

For the purposes of this research twelve test samples were created (Table 1.) using the Adobe Illustrator application. The test samples were based on the Ehrenstein Model - a specific geometric structure consisting of an octagonal system involving gridlines formed by overlapping different color combinations of the primary stimulus.

The color lines on each test sample were combinations of primary colors of additive (red, green and blue) and a subtractive synthesis (cyan, magenta and yellow) as an insert segment of the primary stimulus.

Table .1 Color Combinations of Test Samples

Tests Samples	Inserted Segment Color	Surround Color
1	red	"black"
2	green	"black"
3	blue	"black"
4	cyan	"black"
5	magenta	"black"
6	yellow	"black"
7	red	cyan
8	green	magenta
9	blue	yellow
10	cyan	red
11	magenta	green
12	yellow	blue

"Black" is used as the surround color for the primary stimulus in one instance (Figure 1.) together with colors that are complementary to the color of the inserted segment of the primary stimulus, which are used in a second instance (Figure 2.). The background of the entire primary stimulus is a "white" media color.

When creating test samples a CMYK color scheme was used. A bitmap (*.psd) file format was used. The test samples were printed on a machine calibrated for digital printing - "Epson StylusPro 7900 HDR" - using a liquid toner principle (Epson UltraChrome HDR ink). Rasterization and printing were completed using a "GMG ColorProof" application with an absolute ICC colorimetric rendering method.

The impact of different media was analyzed: the printing surface (GMG ProofMedia - Proof paper Gloss) and the LCD display (HP DreamColor LP2480zx). The measurements were taken under three different CIE standard light sources ("Daylight" D65, "Cool White Fluorescent Light Source" CWF F2 and "Artificial Light" A).

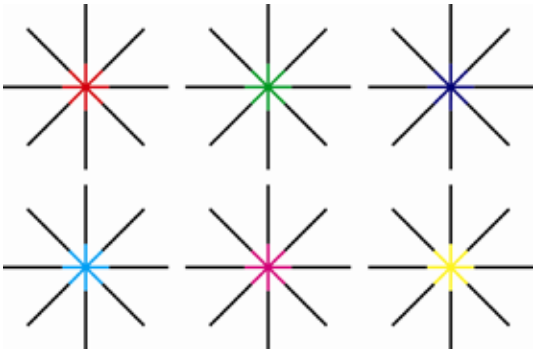

Figure 1 Test Samples with a "Black" Surround

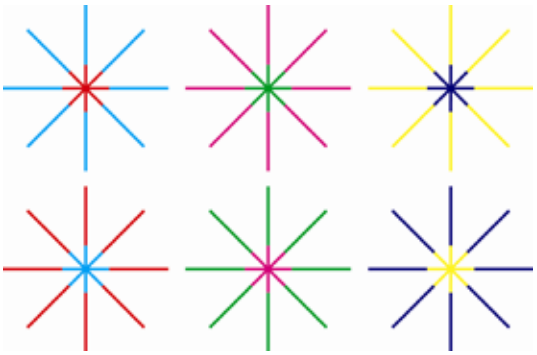

Figure 2 Test Samples with Complementary Color Surrounds

2.2 Results and Discussion

These graphical representation of the calculation method applied to changes of perceptual color attributes is, in accordance with set research target parameters, given in line diagrams in Figures 3 – 14. Some of these diagrams give a comparative overview of the change of a specific perceptual color attributes due to the standard light sources (D65, CWF and A) for the six colors of the insert segments (red, green, blue, cyan, magenta and yellow), the default media (printed images and LCD display) and the specific background color ("black" or its complementary color).

Lightness Differences ΔL^*

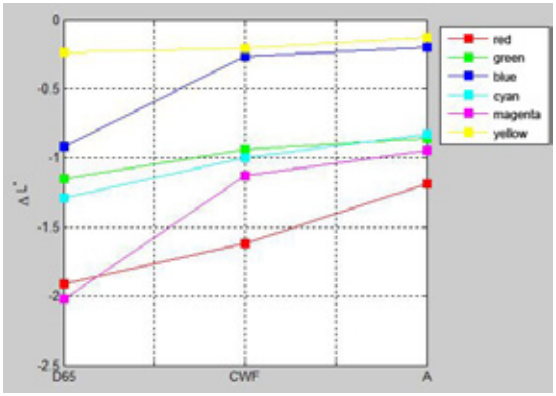

Figure 3. Lightness Differences on a Printed Images by "Black" Surround Color

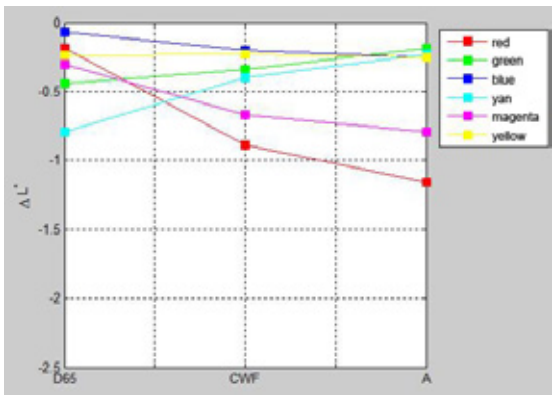

Figure 4. Lightness Differences on a Printed Images by Complementary Surround Color

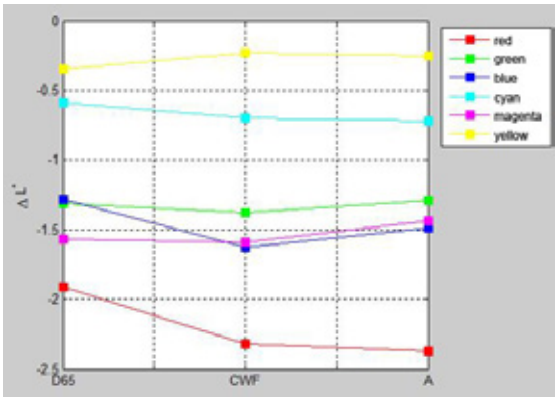

Figure 5. Lightness Differences of the LCD Display by "Black" Surround Color

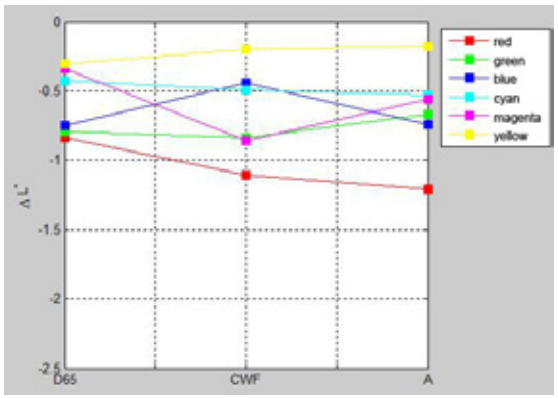

Figure 6. Lightness Differences of the LCD Display by Complementary Surround Color

Figures 2 - 6 show that in all test samples and for all the research parameters the results showed negative value of lightness differences ΔL^*. This implies that the measured stimulus (the color spreading into effect) is darker than the reference stimulus (background color, medium) [13].

Lightness differences values ΔL^* in most incidents are more pronounced for the "black" surround color (value changes in the lightness range for most cases are $\Delta L^* = -2 - 0$) in relation to the complementary surround color (value changes in the lightness range for most cases is $\Delta L^* = -1 - 0$).

The biggest lightness differences were in most cases observed for the Ehrenstein sample red insert segment, regardless of light source, surround color or media. The least lightness differences were in most cases observed for yellow, regardless of light source, surrround color or media. This corresponds with the fact that the yellow color is characterized by high lightness and the lightness differences of yellow color compared to the lightness of the "white" color surround, is the smallest.

The LCD display, as a medium, shows the most uniformed change in lightness if light source variable is taken into consideration. This result corresponds with the established fact that this is an alternative medium in which, mixing of light stimulus occurs without any modulation of individual color components prior to entering the human eye.

Chroma Differences ΔC^*_{ab}

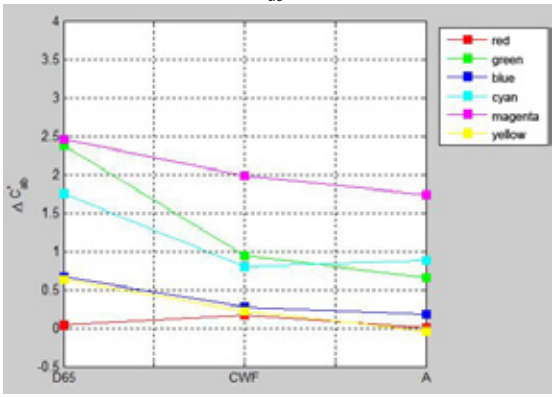

Figure 7. Chroma Differences on a Printed Images by "Black" Surround Color

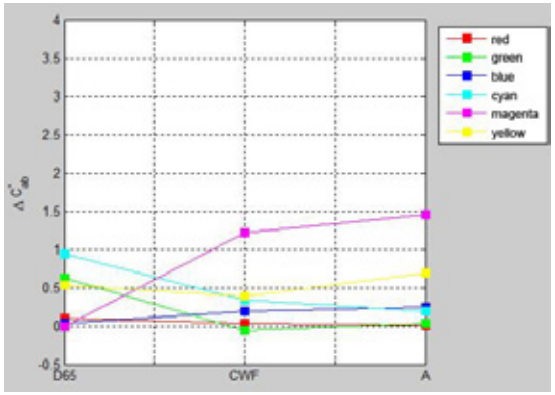

Figure 8. Chroma Differences on a Printed Images by Complementary Surround Color

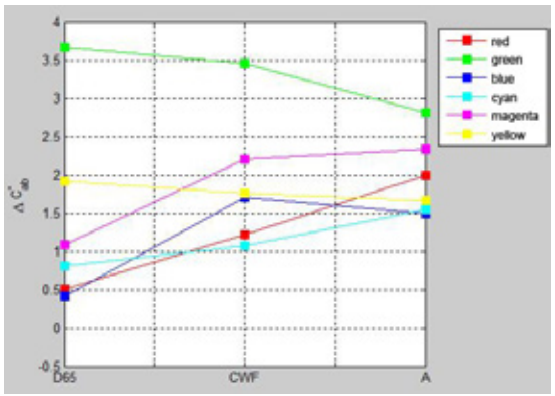

Figure 9. Chroma Differences of the LCD Display by "Black" Surround Color

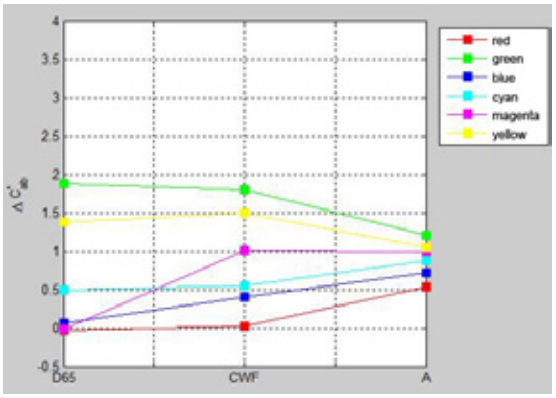

Figure 10. Chroma Differences of the LCD Display by Complementary Surround Color

A graphic display of chroma differences ΔC^*_{ab} in a manifested neon color spreading effect is given in Figures 7 – 10. These Figures show that the values of chroma differences are expected to be positive, and in a few cases there are minor deviations which are not statistically significant (values from -0.02 to -0.06). A positive value of a chroma differences indicates higher induced color chroma in the manifested neon color spreading effect in relation to the surface (medium) chroma.

Chroma differences values range from ΔC^*_{ab} = 0 – 3.66. Larger chroma differences can be seen in LCD displays used as media compared to a printed images used as a medium.

Chroma differences is generally more pronounced in "black" color surround in relation to complementary surround color for attributed colors of inserted segments. This ratio is higher in subtractive media (printed images) than the additive medium (LCD display). In case of a yellow color of inserted segments a uniform chroma changes in both the surround colors may be observed.

The minimum chromatic differences of values were observed in the red insert segment. The red insert segment showed a slightly higher chroma differences with an A light source and an LCD display.

The highest values of chroma differences were observed in the magenta and, in particular, green insert segments for which, with the D65 light source the change was almost twice of other insert segment colors (for "black" surround color on the LCD display).

Hue Differences ΔH^*_{ab}

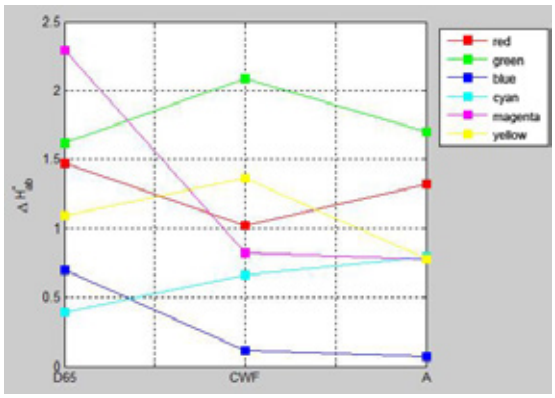

Figure 11. Hue Differences on a Printed Images by "Black" Surround Color

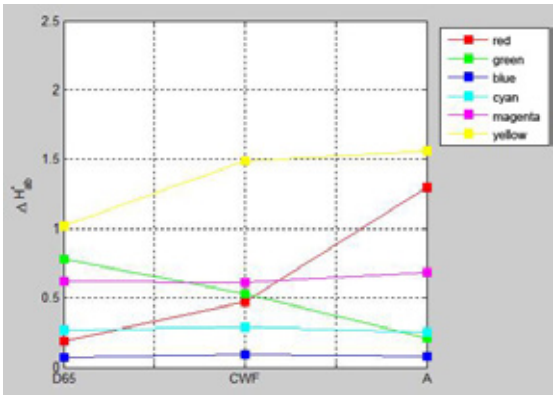

Figure 12. Hue Differences on a Printed Images by Complementary Surround Color

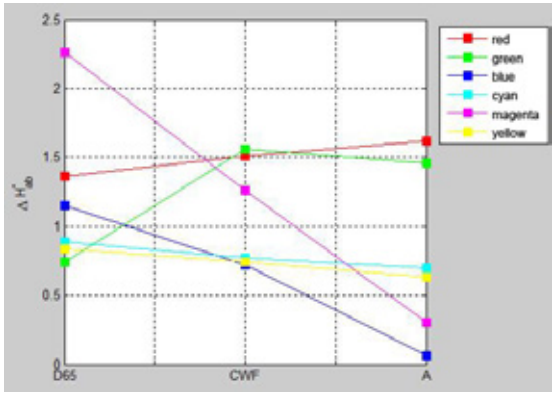

Figure 13. Hue Differences of the LCD Display by "Black" Surround Color

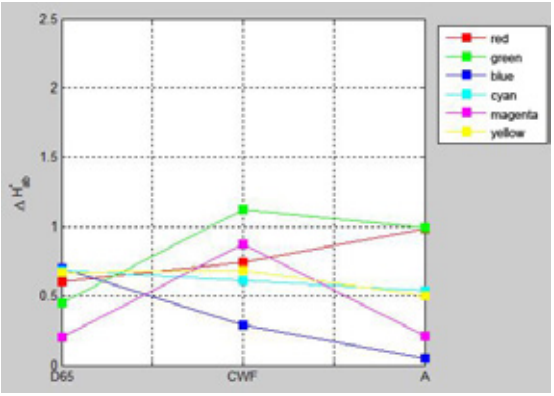

Figure 14. Hue Differences of the LCD Display by Complementary Surround Color

The results show that the incidence of color shift is least in terms of changes of a hue differences. Figures 9 - 12 show the changes of tone values for induced, extended color due to the manifested neon color spreading effect.

The calculated values of tone changes ΔH^*_{ab} range from ΔH^*_{ab} = 0 – 2.29. The lowest recorded values are in blue insert segments, which was earlier previously attributed to the eye's slowness to process the color blue. On the LCD display these values for the color blue are slightly higher when compared to other colors of the inserted segment.

The highest changes in color hue values can in most cases be seen in green, magenta and red colored insert segments.

A more significant change in the color hue of the "black" surround was identified in relation to the complementary surround color. The difference was almost double on printed images than on the LCD display where the difference is negligible.

Certain regularity in the change of color hue ΔH^*_{ab} was not observed in relation to individual light sources.

3 Conclusion

Through a qualitative analysis of illusory color appearance shifts in manifested neon color spreading effect observed through a change of the perceptual attributes of color it was determined that the error in color perception mostly related to the error in the perception of chroma differences ΔC^*_{ab} and an error in lightness differences ΔL^* perception. An error in hue differences ΔH^*_{ab} perception was generally lower than in the previous stated attributes.

The resulting values of changes for each perceptual attributes of color are consistent with the positional averages of the color differences ΔE^*_{94} which is an indicator of the researched effect intensity presented in published papers [10, 11 and 12].

References

1. Hunt, R. W. G., (1995), *The reproduction of Colour in Photography, Printing and Television*. Fountain Press, Tolworth, England.
2. Sueeprasan, S., Luo, M. R., Rhodes, P. A. (2001) Investigation of colour appearance models for illumination changes across media, *Color Research & Application,* 26 *(6)*, 428–435.
3. Milković, M., Zjakić, I., Vusić, D. (2010), *Kolorimetrija u multimedijskim komunikacijama.* Veleučilište u Varaždinu, Varaždin, Croatia
4. Goldstein, E. B. (2010), *Encyclopedia of Perception.* SAGE Publication, London, England.
5. Pridmore, R. W. (2011) Complementary colors theory of color vision: Physiology, color mixture, color constancy and color perception, *Color Research & Application,* 36 *(6)*, 394–412.
6. Milković, M., Bolanča, S., Mrvac, N., Zjakić, I. (2006) The influence of standard rendering methods on the manifesteted intensity of the chromatic induction effect, *Technical gazette,* 13 *(1-2)*, 5-13.
7. Milković, M., Mrvac, N., Matijević, M. (2010) Evaluation of the chromatic assimilation effect intensity in Munker-White samples made by standard methods of rendering, *Technical gazette,* 17 *(2)*, 163-172.
8. Milković, M., Mrvac, N., Vusić, D. (2011) Evaluation of the chromatic adaptation effect intensity by "tuning" the desaturated achromatic reproductions produced in offset, *Technical gazette,* 18 *(4)*, 519-528.
9. Milković, M., Mrvac, N., Vusić, D. (2009), *Vizualna psihofizika i dizajn.* Veleučilište u Varaždinu, Varaždin, Croatia.
10. Vusić, D., Milković, M., Mrvac, N. (2012) The influence of the primary color stimuli selection on the neon color spreading, *TTEM - Technics Technologies Education Management,* 7 *(1)*, 81-87.

11. Vusić, D., Mrvac, N., Milković, M. (2011) The neon colour spreading efect in various surround ambient conditions, *Technical gazette,* 18 *(2)*, 219-225.
12. Vusić, D., Tomiša, M., Milković, M. (2014) Determination of the Influence of Media on the Neon Color Spreading, *Technical gazette,* 21 *(4)*, 807-814.
13. Malacara, D. (2002), *Color Vision and Colorimetry: Theory and Applications.* Spie Press, Washington, USA.
14. Braun, K. M., Fairchild, M. D., Alessi, P. J. (1996) Viewing techniques for cross-media image comparisons, *Color Resarch and Application,* 21 *(1)*, 6–17.

This page was left blank intentionally!

Offset Print Analysis with Mathematical Regression Model

[1]Nandakumar M., [2]Bose N.

[1] Arasan Ganesan Polytechnic College, Sivakasi, India

[2] Mechanical Engineering, Mepco Schlenk Engineering College, Sivakas, Indiai

Abstract

The objective of this study is to analyze and compare the print quality by offset printing process on uncoated paper for matching the quality on par with ISO 12647 standards. A standard test form that contains different control strips for densitometric and colorimetric measuring has been used to define the optical density and color difference of the main process ink colors like cyan, magenta, yellow and black while printed on four-color Heidelberg CD102 sheet-fed offset printing press. The results are important from scientific and practical point of view. By applying the regression analysis methods, the correlation between the optical density deviations ΔD from the optimal values and color difference ΔEab represented by the following regression model of Quadratic equation: $\Delta Eab = a + b\Delta D + c\Delta D^2$ ($y = a + bx + cx^2$) has been ascertained. By using the mathematical regression model, identification of the suitable values of every color on the output in offset printing, can be easily done. The experimental result of print density and LAB values on uncoated paper is matching with ISO 12647-2 Graphic technology – process for the production print.

Key words: Print Quality, Offset Printing, Substrate, Optical Density, Dot Gain, Color Difference, Color Deviations, Regression Model, Control strips.

1. Introduction

The basic principle of offset printing is simple: ink and water do not mix. When the metal plate is exposed, an ink receptive coating is activated at the image area. On the press, the plate is dampened; initially by water rollers, then by ink rollers. The ink adheres to the image area and the water adheres to the non-image area. As the cylinders rotate, the image is transferred to the rubber blanket. The substrate passes between the blanket cylinder and the impression cylinder, where the image is transferred onto the substrate [1]. A great number of quality parameters are defined in the International standards. In offset printing process we operate with parameters like ink quantity, registration of colors, water/ink balance and pressure in printing zone [2]. Uncoated papers are more absorbent of ink than a coated paper. It is generally not as smooth as coated paper and tends to be more pored. These pores contribute to rapid ink penetration and large pores act as the solvent storage. Most types of uncoated paper are surface sized to improve their strength [3]. ISO 2846-1 Graphic technology color as well as transparency of ink sets for four color printing is the internationally recognized standard for offset lithographic printing processes [4]. ISO 12647-2 is the only official international printing standard which specifies a number of process parameters to be applied when preparing color separations for four color offset printing by means of four-color offset lithographic processes [5].

2. Experimental Setup

This paper aims at arriving a mathematical analysis and equation on relating the print density and color parameters printing on uncoated paper by offset printing process. Standard color control strips and elements of solid patches for Cyan, Magenta, Yellow, Black, two color overprint patches, 40% and 80% dot gain patches, slur/doubling control elements, registration marks. During the experiments CtPlates four color positive working printing plates,

TOYO-Leoman process inks, 110 g/m^2 uncoated papers and four color sheet-fed Heidelberg CD 102 were used.

A spectrophotometer/densitometer of type Xrite Spectro-Eye has been used for measuring of optical density and the color characteristics in the CIE Lab color space. Average color characteristics of used papers measured on five different places were in accordance with ISO12647-2 tolerances L±3, a±2, b±2. A series of samples were characterized by gradual smooth changes of ink quantity – from under-inking to over inking. In order to express the analytical dependence between ΔD and ΔEab, it is necessary to apply mathematical modeling, regression analysis and statistical analysis of experimental data, taking into consideration the deviation and variation tolerances from optimal inking for C, M, Y and K. It was determined, that the experimental fitting curve is a parabola, described with the formula: $y = a + bx + cx^2$ in this specific case $\Delta Eab = a + b\Delta D + c\Delta D^2$.

3. Results and Discussion

Density measurements of solid ink patches were used to monitor the ink film thickness applied during a press run. In comparing two printed sheets, density readings should be within 0.05 units, when measured on a Spectrophotometer, for meaningful print quality assessment [6]. The density value of offset printing on uncoated paper was measured with Xrite SpectroEye spectrophotometer. The measured density value for different colors of C, M, Y and K for uncoated paper is given in Fig. 1.

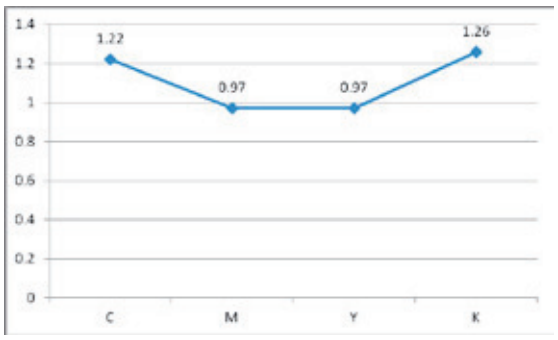

Fig. 1. Density values of uncoated papers

The solid ink density is a function of the percentage of light reflected. From Fig. 1 it is observed that reflection density of the offset printed sheets on uncoated paper of Cyan is 1.22, for Magenta 0.97, for Yellow 0.97 and for Black 1.26.

3.2 Color parameters CIE LAB values

Assessment of color is more than a numeric expression. Usually it's an assessment of the color difference delta from a known standard. CIELAB is used to compare the colors of two objects. Given the ΔL* Δa* Δb* values, the total difference or distance on the CIELAB diagram can be stated as a single value, known as ΔE*ab [7].

$$\Delta Eab = \sqrt{(L_2 - L_1)^2 + (a_2 - a_1)^2 + (b_2 - b_1)^2}$$

The CIE LAB values measured in offset printing of uncoated paper for different color inks of C, M, Y and K using Xrite spectrophotometer is given in Table 2 & 3 and graphically represented in Fig. 2.

It is observed from the Table 1 that the color difference of cyan ΔEab is 2.36, magenta ΔEab is 1.78, Yellow ΔEab is 2.64 and black ΔEab is 0.36. The deviation tolerance as per ISO standard for offset printing of each color is 5 and the differences are within the prescribed value. Hence the LAB value of uncoated paper shows equally good quality of color reproduction compared with ISO standard value. It is observed from the Table 2 that the color difference of Magenta on Yellow print ΔEab is 2.06 for Cyan on Yellow color overprint ΔEab is 2.06 and for Cyan on Magenta overprint ΔEab is 2.30. The color differences are within the range of 5 as represented graphically in Fig. 2. Hence the consistency of the print quality is assured in uncoated paper.

The plotted values of CMYK are not deviating from the OK print of the production run samples color values. The plotted readings of cyan, magenta, yellow and black production prints optical density values are within the variation tolerance as specified in ISO-12647 standard. The half of 4 is 2 for cyan, magenta and black colors. For the yellow color it is 2.5 and the variation tolerances are acceptable. The regression model for cyan, magenta, yellow and black colors optical density ΔD against the color parameters ΔEab is within the tolerance value.

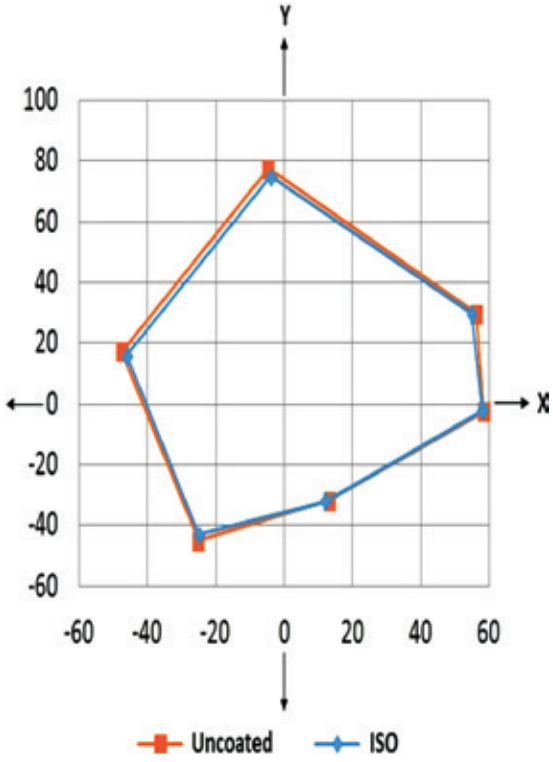

Fig.2 LAB values of uncoated paper [X axis CIELAB red-green coordinate a*] [Y axis CIELAB yellow-blue coordinate b*]

Table 1 LAB Values – for process colors C, M, Y and K on uncoated paper

Color		ISO	Uncoated	ΔEab
C	L*	58.0	59.2	2.36
	a*	-25.0	-25.13	
	b*	-43.0	-45.03	
M	L*	54.0	55.67	1.78
	a*	58.0	58.38	
	b*	-2.0	-2.5	
Y	L*	86.0	87.02	2.64
	a*	-4.0	-4.62	
	b*	75.0	77.36	
K	L*	31.0	31.3	0.36
	a*	1.0	1.2	
	b*	1.0	1.04	

Table 2 LAB Values – for additive colors R, G and B on uncoated paper

Color		ISO	Uncoated	ΔEab
R (M+Y)	L*	52.0	53.60	2.06
	a*	55.0	56.21	
	b*	30.0	29.72	
G (C+Y)	L*	52.0	52.84	2.06
	a*	-46.0	-47.39	
	b*	16.0	17.27	
B (C+M)	L*	36.0	37.93	2.30
	a*	12.0	13.22	
	b*	-32.0	-31.74	

4. Mathematical modeling to characterize solid ink density and color parameters

Mathematical modeling describes the different aspects of the real world, their interaction, and their dynamics through mathematics. Mathematical models also offer new possibilities to manage the increasing complexity of technology [8]. In this paper, a mathematical model is derived to have a deeper understanding of the relationship between the ink density and color values which determine the print quality on uncoated paper. The ink density ΔD for different values of ΔEab were calculated for determining a mathematical relationship between them to:

i. predict the value of ΔEab based on the value of ΔD
ii. explain the impact of changes in the values ΔEab on the values of ΔD. A regression model is applied to find the relationship between the ink density and color values.

Out of the two variables density variation ΔD and color difference ΔEab, ΔEab is considered as the dependent variable and ΔD as the independent variable. Using regression model, it is studied that changes in the values of dependent variable are resulted by the changes in the values of independent variable. Regression model polynomial parabola curve fit is used in this paper to arrive the mathematical model. The relationship between ΔD and ΔEab is represented by the polynomial parabola fit is given by $\Delta Eab = a + b\Delta D + c\Delta D^2$. Fitting a model means obtaining the values of the parameters a, b and c on the basis of collected observations on ΔD and ΔEab.

5. Analysis of the regression model and Discussion

The OriginPro 8 SR4 version software is used in this research for curve fitting using regression analysis to find the relationship between ink density ΔD and color parameters ΔEab. Origin is an industry-leading scientific graphing and data analysis GUI software developed by OriginLab®. Curve fitting is one of Origin's most powerful and most widely used analytical methods. Origin provides tools for linear and nonlinear curve fitting. The output data of printed sheet results are assessed by feeding the readings of Cyan, Magenta, Yellow and Black density readings ΔD and ΔEab color differences to find the best fit regression model. A regression model is first developed, and then the best fit parameters are estimated using the least-square method. Finally, the quality of the model is assessed using hypothesis tests of R^2, T-value and F-value of ANOVA to ascertain the fitness of the regression model. The regression model equation, estimated R^2, T-statistics and F-test ANOVA of the data for uncoated is shown in Table 3 and plots of the CIE LAB values of C, M, Y and K are shown in Fig. 3.

In X axis the ΔD optical density and Y axis ΔEab color parameters are taken, the readings were fitted in the regression line for all four process colors. The individual measured values of ΔD and ΔEab of Cyan, Magenta, Yellow and Black readings were plotted in the regression equation shown in the graph. The different readings of printed samples were assessed for their quality reproduction and OK print samples were considered for the analysis of density color difference on uncoated paper.

Table 3 Regression Model for Uncoated paper

Ink	Mathematical model (Regression)	R2	F (ANOVA)	T-statistics
Cyan	ΔE = 1.23899 -9.48388 ΔD + 599.06023ΔD ^{2}	0.90552	241.84096	7.38924
Magenta	ΔE = 1.20154 + 1.25273 ΔD + 1155.03714ΔD ^{2}	0.94968	454.47028	7.35956
Yellow	ΔE = 1.74978 + 0.94668 ΔD + 1566.22125ΔD ^{2}	0.93953	353.20034	7.07146
Black	ΔE = 0.63296 -1.70439 ΔD + 215.49149ΔD ^{2}	0.95568	785.03328	8.9765

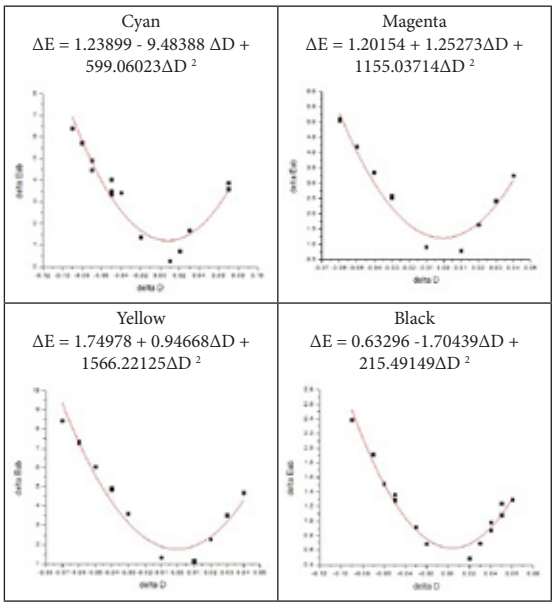

Fig. 3 Graph showing the scatter plot and fitted lines for uncoated paper

In the regression model $y = a + bx + cx^2$, 'a' is the y-intercept and 'b' is the slope. From these experimental values and mathematical models it is studied that the slope is normal for all CMYK process colors. It shows that there is a linear relationship between optical density and color values.

5.1 Goodness-of-fit

Linear regression calculates an equation that minimizes the distance between the fitted line and all of the data points. Technically, ordinary least square regression minimizes the sum of the squared residuals [9]. In general, a model fits the data well if the differences between the observed values and the model's predicted values are small and unbiased. The fitness of the model can be proved using the following parameters:

1. Coefficient of determination (R^2)
2. t-test statistics
3. F-test (ANOVA)

5.2 Coefficient of determination

The goodness of the fitted model is studied by calculating the Coefficient of determination R^2. R^2 is a statistical measure showing the closeness of the data to the fitted regression line. R^2 is the

percentage of the response variable variation that is explained by a linear model.

R^2 = Explained variation / Total variation

$$R^2 = \frac{\sum_{i=1}^{n}(y_i - \bar{y})^2}{\sum_{i=1}^{n}(y_i - \bar{y}_i)^2}$$

R^2 is always between zero and one. Zero indicates that the model explains none of the variability of the response data around its mean and One indicates that the model explains all the variability of the response data around its mean. In general, the higher the R-square, the better the model fits the data. From Table 3, it is clearly noted from the experimental results that for uncoated paper R^2 is calculated for cyan is 0.90552, Magenta is 0.94968, Yellow is 0.93953 and for black it is 0.95568. As stated earlier the R^2 for uncoated paper values of CMYK are very close to the 1 and hence the mathematical models arrived are considered to be fitted model.

5.3 t-Test for the slope

The t-value is a statistic test that measures the difference between an observed sample statistic and its hypothesized population parameter in units of standard error. A t-test compares the observed t-value to a critical value on the t-distribution with (n-1) degrees of freedom to determine whether the difference between the estimated and hypothesized values of the population parameter is statistically significant.

For the fitted model, the hypothesis is tested. The slope is zero against H_o:b=0 against H_a:b≠0 is tested [10]. The test statistics is

$$T_c = \frac{\hat{b}}{\sqrt{\frac{\sum_{i=1}^{n}(y_i - \hat{y})^2}{(n-2)\sum_{i=1}^{n}(x_i - \bar{x})^2}}}$$

The t-test value of uncoated paper results for Cyan, Magenta, Yellow and black were computed and entered in Table 3. The T-statistics for cyan is 7.38924, Magenta is 7.35956, Yellow is 7.07146 and for black it is 8.9765. The T-statistics value at 5 % level of significance and 13 degree of freedom, the critical value referred from the t- distribution Table minimum is 2.160. It is verified from the computed T-Values of CMYK are higher than 2.160. Therefore, at 5% level of significance the null hypothesis is rejected for uncoated paper of all process colors of Cyan, Magenta, Yellow and Black. Hence it is concluded that there is an evidence of linear relationship between the optical density deviations ΔD from the optimal values and color difference ΔEab of print quality on uncoated paper.

5.4 F-Test (ANOVA)

F-test can be used as an alternative for t-test for linearity. In F-test also, the hypothesis H_0 : b = 0 is tested. This test is based on the concept of partitioning the total variability into explained variability and unexplained variability.

$$F = \frac{\sum_{i=1}^{n}(\hat{y}_i - \bar{y})^2\, x}{\sum_{i=1}^{n}(y_i - \hat{y})^2}$$

An F-test is any statistical test in which the test statistic has an F-distribution under the null hypothesis. It is most often used when comparing statistical models that have been fitted to a data set, in order to identify the model that best fits the population from which the data were sampled. Exact "*F*-tests" mainly arise when the models have been fitted to the data using least squares.

The F-test value for uncoated paper of Cyan, Magenta, Yellow and black were computed and entered in Table 3. The F-statistics for the uncoated paper for cyan is 241.84096, for Magenta 454.47028, for Yellow 353.20034 and for black 785.03328. F-value at 5% level of significance and (1, 13) degree of freedom, the critical value using F distribution table is 4.67 which is lesser than the computed values shown in Table 3. Therefore, at 5% level of significance the null hypothesis is rejected and concluded that there is an evidence of linear relationship between the optical density deviations ΔD from the optimal values and color difference ΔEab in print quality on uncoated paper.

6. Conclusion

The experimental research was carried out in real production conditions. The deviation and variation tolerances from optimal inking density values from offset printing outputs on uncoated paper was thus determined, taking into consideration the human optical perception and the specific production conditions. The obtained results for deviation and variation tolerances can be used in practice for quality control of printing process. The experimental

results demonstrate that there is correlation of print density and LAB values of the inks on uncoated paper matching with International Standard ISO 12647-2 Graphic technology - Process control for the production of prints. The mathematical regression model also evidently confirms the linear relationship between the optical density deviations ΔD and color difference ΔEab of print quality on uncoated paper by offset printing process. Mathematical regression model can be developed for the specific printing press condition positively and applied in practice effectively for determining quality on sheet-fed offset presses.

Acknowledgement

The authors would like to thank
Mr. Vashikaran Rajendrasingh, Bell Printers, Sivakasi for providing all facility for carrying out our print experimental works.

References

1. Raymond N. Blair, The lithographers manual, Seventh edition, pp. 1:9 – 1:11.
2. Helmut Kipphan, Handbook of Print Media, Springer, Heidelberg, pp. 206-354.
3. NIIR Board of consultants & engineers, Modern technology of pulp, paper and paper conversion industries, pp. 356-410.
4. International Standard, ISO2846-1, Graphic technology Color and transparency of ink sets for four-color-printing.
5. International Standard ISO 12647-2, Graphic technology - Process control for the production of halftone color separations, proof and production prints – Part 2: Offset lithographic processes, pp 1-19.
6. A Guide to Understanding Graphic Arts Densitometry, X-rite manual, pp 1-11.
7. Roy S. Berns, Billmeyer and Saltzman's Principles of Color Technonogy, Third edition, 2000, Wiley-Inter science Publication, pp. 107-130.
8. C.F.Jeff Wu, Michael Hamada, Experiments – Planning, Analysis and Parameter design Optimization, Wiley India, 2002, PP. 135-142.
9. Clive L. Dyn, Principles of Mathematical Modeling, 2nd edition, Academic Press, 2004, pp. 3-12.
10. C.R.Kothari and Gaurav Gard, Research Methodology Methods and Techniques, Third edition, New Age International Publishers, 2014, pp. 312-331.

Energy Efficient Cooperative Spectrum Sensing in Cognitive Radio Networks Using Distributed Dynamic Load Balanced Clustering Scheme

Muthukkumar R., Manimegalai D.

National Engineering College, Tamil Nadu, India.

mkumarnec@gmail.com

Abstract

Cognitive Radio (CR) is a promising and potential technique to enable secondary users (SUs) or unlicenced users to exploit the unused spectrum resources effectively possessed by primary users (PUs) or licenced users. The proven clustering approach is used to organize nodes in the network into the logical groups to attain energy efficiency, network scalability, and stability for improving the sensing accuracy in CR through cooperative spectrum sensing (CSS). In this paper, a distributed dynamic load balanced clustering (DDLBC) algorithm is proposed. In this algorithm, each member in the cluster is to calculate the cooperative gain, residual energy, distance, and sensing cost from the neighboring clusters to perform the optimal decision. Each member in a cluster participates in selecting a cluster head (CH) through cooperative gain, and residual energy that minimises network energy consumption and enhances the channel sensing. First, we form the number of clusters using the Markov decision process (MDP) model to reduce the energy consumption in a network. In this algorithm, CR users effectively utilize the PUs reporting time slots of unavailability. The simulation results reveal that the clusters convergence, energy efficiency, and accuracy of channel sensing increased considerably by using the proposed algorithm.

Keywords: Cognitive radio (CR), cooperative spectrum sensing (CSS), clustering, energy efficiency.

1 Introduction

Cognitive Radio (CR) facilitates unlicensed or secondary users (SUs) to utilize the unused spectrum resources (called spectrum holes or white spaces) effectively owned by licenced or primary users (PUs) [1, 2]. Spectrum sensing is the prime role of CR network for spectrum investigation to determine the white spaces and to prevent PUs from harmful interference. The probability of detection (*Pd*) and the probability of false alarm (*Pf*) are two important performance metrics used to compute the consistency of spectrum sensing schemes for identifying the accessibility or otherwise of white spaces. However, some specific impairment of propagation is shadowing, receiver uncertainty, interference, and multipath fading in communication channels that affect the functioning of PU detection [3].

CSS is another technique to overcome the above problems in CR network, to improve the PU detection performance [4]. This technique involves directing multiple CR users to send their sensing result and a cooperative decision is made about the availability of unused spectrum or white spaces. It also enhances the PU detection probability through the study of multiuser's diversity. CSS also gives a better sensing performance, but increase communication overhead that take more energy consumption as well as further delays of sensing and reporting, especially in larger networks [5]. It can be minimised by a partitioning of more CRs to formulate a cluster.

In CR ad hoc network, clustering is a key mechanism of topology management that organizes nodes into the logical group of nodes (or cluster) to offer network-wide performance improvement. Each cluster contains a cluster head (CH) while other nodes in a cluster are referred as member nodes (MN). In a cluster, the CH also acts as controller and executes diverse functions, like channel sensing coordination, routing and aggregation of data. Further, it offers inter-cluster communications in which each CH in a cluster communicates with its

neighbour CH and FC. Each cluster, the MNs determines any events and sends to their CH through either multi-hop or single-hop routing through intra-cluster communications

Various schemes have been designed for minimizing the energy consumption. Qing et al. [6] proposed a Distributed Energy Efficient Clustering (DEEC) protocol. In this approach, nodes autonomously selected as cluster heads based on initial energy (En_I) and (En_{Re}). A node should not have enough energy level, it does not participate CH selection. Smaragdakis et al. [7] proposed a Stable Election Protocol (SEP) to extend the time duration before the first dead node occurs in a heterogeneous network. In this approach, complex and normal nodes are renowned when selecting the cluster head. Younis et al. [8] proposed Hybrid Energy-Efficient Distributed (HEED) protocol. In this approach, CH selected with higher En_{Re} level and more number of neighboring nodes. Rauniyar et al. [9] proposed Energy Efficient Clustering Scheme based on CSS (ECS). In this approach, a spectrum aware pair-wise coupling is used for grouping the nodes into clusters. ECS scheme does not sufficiently address the mobility of nodes in a network. Moreover, all of these clustering schemes use a fixed channel allocation policy and cannot handle mobility of nodes in a network. Therefore, the mobility of nodes is very much essential in CR ad hoc networks to enhance the CSS.

We proposed a novel approach, distributed dynamic load balanced clustering (DDLPC) for enhancing CSS in CR ad hoc network. Its prime aim is to enhance the energy efficiency in CR networks. Our work is distinguished from above mentioned schemes; this DDLPC achieves better sensing capability and prolong the network lifetime. The contributions of this works are outlined as follows:

- DDLPC algorithm is proposed to enhance CSS in CR ad hoc network, which consists of three stages: Cluster formation, CH selection, and re-clustering stages.
- First, the cluster can be formulated using *cooperative footprint decision* (CFD) model. After formation of the cluster, a CH is selected.
- During the CH selection, each node independently calculates their *coop-footprint cost* (CFC) that includes cooperative gain (C_g) and residual energy (En_{Re}). Both C_g and En_{Re} is determined after the first round. All the nodes share the CFC with their neighbors. The node with highest CFC becomes a CH.
- The re-clustering stage deals with mobility or replacement of nodes in a network.
- Through extensive simulation results, we analyse the performance of the proposed DDLPC. The results reveal that the DDLPC outperforms than other schemes in analyzing the clusters stability, network lifetime, energy efficiency, and accuracy of channel sensing.

The rest of the paper organizes five sections. Section 2 summarize related works and emphasizes the dissimilarities between it and proposed work. Section 3 explains our DDLBC in CR ad hoc network in terms of cluster formulation, analysis of clusters stability, network lifetime, energy efficiency, and accuracy of channel sensing. Section 4 presents our simulation results and relevant performance analysis. At last, Section 5 illustrates the conclusions and discusses the future work.

2 Related Works

Energy efficient CSS in CR ad hoc network is a key challenge for several applications. Clustering plays a vital role in providing energy efficiency in CR ad hoc network. Mustapha et al. [2] proposed a clustering algorithm with reinforcement learning (EESA-RLC) to reduce energy consumption and enhance the channel sensing. Yau et al. [10] surveyed the various clustering algorithms to establish *single-hop* or *multi-hop* clusters in CR networks and their metrics. They also addressed the various clustering schemes in CR ad hoc network. The algorithms are categorized by clustering purposes and metrics. Zhang et al. [11] addressed the proper channel assignment policy to each SU in a cluster based CSS and maximized the throughput for all SUs. H Zhang et al. [12] presents distributed spectrum-aware clustering (DSAC) for restricting interference to PUs and also minimize the energy consumption using group-wise constrained clustering. Miah et al. [13] proposed *eigenvalue* detection technique with superposition approach in cluster-based

CSS to attain better detection performance and sense the PUs signal accurately.

Ghorbel et al. [14] presented clear expressions of comprehensive study of *Pd*, *Pf* and cluster based CSS. Sun et al. [15] addressed the grouping all the SUs into some clusters and selecting one user in each cluster to report to the base station and can utilize the user selection diversity to enhance the sensing performance. Wang et al. [16] proposed the clustering mechanism with CSS improved the performance of channel sensing and reduce the computational cost. Bai et al. [17] addressed spectrum efficiency in CR network. In this approach, CR users with adequate information in each cluster will send their sensing results to each CH for decreased the number of sensing bits during spectrum sensing.

Nguyen et al. [18] proposed a frequency division-based parallel reporting mechanism with a selective method that can significantly minimize the energy consumption and reporting time in cluster based CSS. Wang et al. [19] investigate issues of cluster-based CSS in 2-layer hierarchical CR networks with soft data fusion for minimizing the *Pf*. Zhang et al. [20] addressed the distributed clustering algorithm with soft-constraint affinity propagation message passing model for improving the efficiency and robustness of the clusters. Our previous work [21], mobility aware clustering scheme addressed the node behaviors can be estimated in terms of distance, speed, acceleration, and relative velocity with regular intervals. This approach is used to improve the clustering structure and scalability.

Our work is related to that of Qing et al. [6] and Rauniyar et al. [9]. We will compare our work with theirs in the following section. Compared to related work [6, 9, 13, 12, 15, 16, 18-20], our work is distinguished by the type of clustering. We have formulated clustering with MDP algorithm, re-clustering through mobility of users, inter and intra-cluster communication, for a Distributed Dynamic Load Balanced Clustering Scheme. The prime aim of this scheme is to enhance energy efficiency by analyzing the sensing and reporting time of CR users. It also evaluates the re-clustering strategy for the member in a cluster to minimise the energy consumption and prolong the network lifetime. In addition, because our approach is different from those of related work, we assume that it is necessary to determine the re-clustering with mobility if MN moves from one cluster region to other. In a simulation result, we obtain different analyses of clustering and mobility of nodes strategies to meet the better sensing capability in CSS. As a novel contribution, this is the first work to use a Distributed Dynamic Load Balanced Clustering Scheme for enhancing the energy efficiency in CR networks.

3 DDLBC Scheme

3.1. Clustering and Cluster Head Selection

We consider CSS in a distributed CR ad hoc network with M SUs, N PU channels and a fusion centre (a cognitive base station). Each channel is exclusively occupied by the PU. However, each SU can opportunistically sense the channel for detecting the presence or absence of PUs in the channel. The *M* SUs are grouped into a number of clusters. In a cluster, SU is also referred as member node (MN). Each member is actively participating in selecting one cluster head (CH). The prime aim of CH is to gather all the sensing result from MNs and aggregate the result. The CH communicates to FC with the best sensing result to reduce the energy consumption. Moreover, each member calculates their CFC after the first round. The CFC can be calculated as:

$$CFC = \frac{En_{Re} \quad Ch_v}{En_{max}} \tag{1}$$

Where En_{max} indicates the *maximum energy* of the SU and Ch_v represents the *number of vacant channels*.

Then, each member has exchanged CFC information to other nearby members in CR network. The CH is selected according to the largest CFC value. The cluster based CSS in CR ad hoc network system is illustrated in Fig. 1. However, the CSS is accomplished through the following stages:

1. Each SU (or MN) in CR network perform the confined spectrum sensing. Each SU gathers the CFC and sends a local observation $\left(Lo_{ob} \right)$ to the CH. The Lo_{ob} is associated to En_{Re} by MDP function φ as

$$Lo_{ob} = \varphi\left(En_{Re} \right) \tag{2}$$

2. Then, CH receives that Lo_{ob} from the SUs in the cluster, and then makes a cumulative cluster decision (Cl_{cc}) according to the certain fusion function (F_δ) . All the CH sends their better decision to the FC.

$$Cl_{cc} = F_\delta\left(Lo_{ob,1}\ ,\ Lo_{ob,2},\ Lo_{ob,3}\ ,\ldots\ldots\ldots\ldots,L\right. \quad (3)$$

3. Finally, the FC makes the final decision (F_D) according to the fusion strategies. The CH and FC make the F_D according to a fusion function ϖ to reduce the interference from the SUs to the PU.

$$F_D = \varpi\ \left(Cl_{cc,1}\ ,\ Cl_{cc,2},\ Cl_{cc,3}\ ,\ldots\ldots\ldots\ldots,Cl_{cc,K}\right. \quad (4)$$

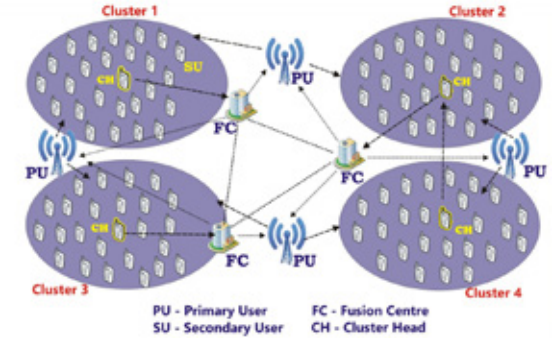

Fig. 1. Cluster based CSS in CR ad hoc network system model

Each SU to choose a communication channel (CC) from the control channel set provided by CH. Assume that, if each SU can discover the presence of PUs in the current CC, to notify the other SU within a cluster when the channel is currently occupied by PU. Even though, we formulate the P_d and the P_f of a cluster with two fusion rules as φ and ϖ .

3.1.1 Formulation of Fusion Decision (∂)

Fusion Decision (∂) for CSS is expressed by two fusion rules, φ and ϖ can be denoted as

$$\varphi: \quad Lo_{ob} = \begin{cases} 1, & En_{Re} > \lambda \\ 0, & otherwise \end{cases} \quad (5)$$

$$\varpi: \quad F_D = \begin{cases} 1, & \sum_{i=1}^{N} Cl_{cc,i} \geq \lambda \\ 0, & otherwise \end{cases} \quad (6)$$

Where each SU in a cluster makes a decision by comparing it's En_{Re} with the threshold value (λ). Then CH for every cluster makes a Cl_{cc} by using an MDP-rule to every Cl_{cc} decision in the particular cluster. Therefore, the P_d and the P_f for the M SUs of the k clusters can be expressed as follows:

$$P_d = P\left(Cl_k > \lambda | H_1\right) = Q\left[\frac{\lambda - \xi(Cl_k \mid H_1)}{\sqrt{\vartheta(Cl_k \mid H_1)}}\right] \quad (7)$$

$$P_f = P\left(Cl_k > \lambda | H_0\right) = Q\left[\frac{\lambda - \xi(Cl_k \mid H_0)}{\sqrt{\vartheta(Cl_k \mid H_0)}}\right] \quad (8)$$

where H_1 and H_0 represent the *presence* and *absence* of PUs signal respectively, ξ and ϑ denotes the *mean* and *variance* of hypothesis test. From (7) and (8), we can obtain the analytical results for the cluster based CSS in CR ad hoc network with *fusion decision* (∂).

3.1.2 Formulation of Energy Fusion Decision (ψ)

Energy Fusion Decision (ψ) for CSS is derived by two fusion rules, φ and ϖ can be denoted as

$$\varphi: \quad Lo_{ob} = En_{Re} \quad (9)$$

$$\varpi: \quad F_D = \begin{cases} 1, & \sum_{i=1}^{N} Cl_{cc,i} \geq \lambda \\ 0, & otherwise \end{cases} \quad (10)$$

where *CH* collects the En_{Re} of all the members in the cluster and then make F_D by comparing it with the value of λ . For the CH of cluster k , the collected En_{Re} can be represented as $Lo_{ob} = \sum_{i=1}^{N} En^k{}_{Re}$. The density function of Lo_{ob} can be determined using the *chi-square distribution* (η) method as:

$$D_f(Lo_{ob}) = \begin{cases} \eta, & H_0 \\ \eta(\rho_k), & H_1 \end{cases} \quad (11)$$

where $\rho_k = \sum_{k=1}^{N}$ is the SNR value at the CH of cluster k . From (11), the P_d and P_f for the M SUs of the k clusters can be described as follows:

$$\begin{aligned} P_f &= P\left(Lo_{ob,i} > \lambda \,|H_0\right) \\ &= \int_{\lambda}^{\infty} \eta \ .\ D_f\left(Lo_{ob,i}\right) \\ &= \frac{\Gamma(\eta,\ \frac{\lambda}{2})}{\Gamma(\eta)} \end{aligned} \quad (12)$$

similarly,

$$\begin{aligned} P_d &= P\left(Lo_{ob,i} > \lambda \,|H_1\right) \\ &= \int_{\lambda}^{\infty} \eta\,(\rho_k).\ D_f\left(Lo_{ob,i}\right) \\ &= \frac{\Gamma(\eta(\rho_k),\ \sqrt{\lambda})}{\Gamma(\eta(\rho_k))} \end{aligned} \quad (13)$$

From (12) and (13), we obtain the analytical results for the cluster based CSS in CR ad hoc network with *energy fusion decision* (ψ).

3.1.3 *Intra-cluster communication*

In *intra-cluster communication,* all SUs in a cluster send their local sensing information to CH thorough the local communication channel. To reduce the energy consumption, choose CH dynamically because CH consumes more energy than MN in a network. However, load balancing approach allows all the MN has equal privileges to become CH to counterbalance the level of energy consumption in a cluster.

Before executing the algorithm that select a CH, the node with enough En_{Re} is selected as CH and remains other SUs cooperate with CH in a cluster. The total energy for *intra-cluster* communication can be determined as:

$$CE_{intra} = (CH = M_i^k) = \sum_{i=1}^{M_k} CE_T(M_i^k) = 2\gamma . CE_R \sum_{i=1}^{M_k} tr^2(M_i^k, M_j^k) \quad (14)$$

where CE_T is a minimum transmission power and $tr^2\left(M_i^k, M_j^k\right)$ denotes the distance between two nodes in a cluster which can be obtained through channel estimation.

Let us consider all MN has equal privileges to become CH, so the average energy for *intra-cluster* communication can be determined as follows:

$$CE_{intra} = \sum_{M=1}^{K} \gamma . CE_R \sum_{j=1}^{M_k} \frac{1}{M_k} \sum_{i=1}^{M_k} tr^2(M_i^k, M_j^k)$$

$$= 2\gamma . CE_R \sum_{M=1}^{M_k} \sum_{i=1}^{M_k} tr^2\left(M_i^k, Cl_{cen}(k)\right) \quad (15)$$

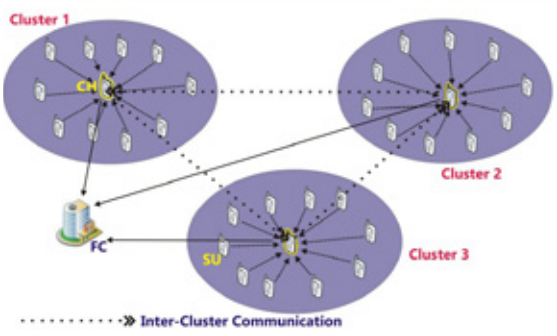

Fig. 2. Inter and Intra-cluster communication model

From (15), we study the shorter distance of intra-cluster can better to reduce the distance between two MNs and their corresponding CH within a cluster. It facilitates to minimise the energy consumption and latency of intra-cluster because of lower communication energy.

2.0.4 *Inter-cluster communication*

In *inter-cluster communication,* a CH within a cluster to collect local sensing information from MNs and formulates a collective sensing information. This collective information is forwarded to FC either through neighboring CH $\left(if\ CH_{i,dist} > tr_{max}\right)$ or straight to the FC $\left(if\ CH_{i,dist} \le tr_{max}\right)$ through the idle channels with maximal transmission power.

Fig. 2 shows the inter-cluster communication model of CR ad hoc networks. In this period, the CH reduces and sends the collective local sensing result to FC. The communication between CH in cluster 1, 2 and 3are represented by dashed arrow and then to FC. The total *inter-cluster* communication energy can be determined as:

$$CE_{inter} = \sum_{M=1}^{K} CE_{Inter-Cluster} = K.\gamma . CE_R tr_{max}^2 \quad (16)$$

The total energy consumption for communication of information can be determined as follows:

$$CE_{CE} = CE_{intra}(i,j) + CE_{inter}$$

$$= \sum_{i=1}^{K} \left\{ \sum_{j=1}^{M_k} \left[\left(CE_T(M_i^k, \beta) + CE_R(\beta) \right) + CE_{i,j}(\beta_{i,j}, Cl_k) \right. \right.$$

$$\left. \left. + CE_{CH}\left(M_i^k, \beta_{i,j}\right) \right] \right\} \quad (17)$$

where β represent the collective information is transmitted to FC and received by FC. Therefore, the total energy consumption of whole network is represented by:

$$CE_{Net} = \sum_{M=1}^{K} CE_{CH}(K) + \sum_{i=1}^{M_k} CE_{MN}(i,j) \quad (18)$$

3.1.5 *Optimal number of clusters*

We consider M SUs and group them into k clusters. With load balancing method, each cluster has balanced level of SUs and each SU is an autonomous cluster. Suppose all M SUs are grouped into only a cluster, the CE_{intra} becomes very large because of large intra-cluster distances. This will give too much energy consumption. So, we need to form the number of optimal clusters carefully with M SUs to minimize the energy consumption in CR ad hoc networks.

In load balancing method, SUs are distributed uniformly and analyse the optimal clusters that

can significantly reduce the energy consumption in CR ad hoc networks. From (14) and (16), the total communication energy is computed approximated as

$$CE_{tot} = \gamma . CE_R \, En_{Re} \left[\sum_{k=1}^{K} \sum_{i=1}^{M_k} {d_{clus}}^2 \left(M_i^k, Cl_{cen}\,(k) \right) \right) + K . 2\gamma . CE_R \, (tr_{max}^2) \quad (19)$$

where γ is loss factor which is used to find out the level of priority for access the channel, CE_R is a minimum reception power, Cl_{cen} is a center of k clusters and tr_{max} is the maximum communication range of each SU.

Suppose, all SUs are distributed uniformly and density functions (£) of each cluster can be determining as follows:

$$En_{Re} \left[\sum_{k=1}^{K} \sum_{i=1}^{M_k} {d_{clus}}^2 \left(M_i^k, Cl_{cen}\,(k) \right) \right) = M \left[\vartheta \left(x_j^k \right) + \vartheta \left(y_j^k \right) \right] = \frac{N . {d_{clus}}^2}{3} \quad (20)$$

where d_{clus} is the average distance of a cluster, x_j and y_j are the coordination points in a network.

There are $\frac{K}{M}$ Sus per cluster through load balancing method and the communication range of each cluster can be determined as ${d^2}_{clus} = \frac{K}{M_£}$. Substitute this value into (19), we get

$$En_{Re}(CE_{tot}) = \gamma . CE_R \left(\frac{M^2}{1.5£\,\mathrm{K}} + K . tr_{max}^2 \right) \quad (21)$$

Obviously, (21) is a rounded function where number of optimal clusters can be determined by assigning *K* value to 0. The number of optimal clusters can be determined as follows:

$$K_{optimal} = \left| \frac{M}{tr_{max} \sqrt{1.5\,£}} + 1.5 \right| \quad (22)$$

From (22), we study the optimal number of clusters provides the better coverage by increasing the number of MNs or maximising the cluster size in a cluster. It can also reduce the large amount of *intra-cluster communication,* mostly during transmission. Furthermore, it minimises overlaps between clusters and can reduce the channel conflict between clusters.

3.1.6 DDLBC algorithm

The following DDLPC algorithm describes the various stages of CSS in CR network.

Initialize ( )
Define each node in a network as disjoint cluster:
$CL_j \left(M_j \right) \leftarrow M_j$
Communication Channel Sensing ( )
$CC_c(n_j), \quad for\ j = 1, 2, 3, \ldots\ldots\ldots . . N$
DDLBC:
a. Node CFC:
$for\ j = 1, 2, 3, \ldots\ldots\ldots . . N\ \ do$
$CFC\ \ Node\_ID$
If ${CC_c}^i \left(M_j \right) = {CC_c}^{i-1} \left(M_j \right)$ **then**
$CFC\ \ Cluster\_ID: CL_j^i \left(M_j \right) = CL_j^{i-1} (M_j)$
else
$CFC\ \ New\ Cluster\_ID$
$CL_j^i \left(M_j \right) = New\ CL_{ID}$
endif
endfor
b. Cluster_CFC:
$For\ k = 1, 2, 3, \ldots\ldots\ldots . . M\ \ do$
$CFC\ \ Cluster\_Size: \left| CL_k^i \right|$
$Control\_Channel: {CC_c}^i (CL_k)$
end for
c. Intra _Cluster _Communication:
$For\ k = 1, 2, 3, \ldots\ldots\ldots . . M\ \ do$
If CFC node_ID $CL_n^r < \left| CL_n^i \right|$ **then**
distance $d\,(CL_k, CL_n) \leftarrow \infty$
else
$d\,(CL_k, CL_n) = \max_{n_j \in CL_k, n_l \in CL_n} d(M_j, M_l)$
end if
Discover neighboring cluster
$ne = \min_{ne \in N_{eiighbor}(k)} d(CL_k, CL_n)$
endfor
d. Inter_cluster _Communication:
CL_k Send $Group\_req$ to CL_n
$if\ \ CL_k$ receives $Group\_res$ as of CL_n then
New Cluster_ID: $CL_{New} \leftarrow (CL_k, CL_n)$
Assign Communication _Channel:
${CC_c}\ (CL_{New}) = |CC_c(CL_k) \cap CC_c(CL_n)|$
end if
e. Re-clustering: Mobility of Node CL_{New} from on cluster to another. Select new Cluster Head ID
goto Communication **Channel Sensing**

The DDLBC algorithm consist of five stages such as *communication channel sensing*, *cluster formation*, *optimal number of cluster selection, intra / inter cluster communication*, and *re-clustering.*

2.0.7 Re-clustering

Re-clustering is necessary in a cluster whenever a communication channel cannot be found, the MN far away from its cluster coverage area because of its mobility, and the current energy

level of CH is very low. Since, MN has mobility which moves from one cluster to other. With stimulated time interval, re-clustering is performed in a network. The time interval plays a vital role during the transmission. If the time interval is set too high, then CHs consume too much amount of energy and subsequently died before the re-clustering. Furthermore, with substandard time takes too much transmission cost.

So, we evaluate En_{Re} of the CH with an agreed threshold, if En_{Re} is lesser than an agreed threshold, it sends re-clustering information to cluster region. Therefore, $Re_{c,CH}$ and $Re_{av,CH}$ are denoted as the residual energy and average energy level of CH. Moreover, the provision of re-clustering is:

$$Re_{c,CH} \leq \Delta\, Re_{av,CH} \tag{23}$$

The MN encapsulates it's Re in the packet while it sends them to the CH. When the packet reaches the CH, it will again compute the average En_{Re} of the cluster. If this value satisfies (24), the CH will send re-clustering message in its cluster region which will cause the *intra-cluster* re-clustering. However, there are K clusters in the network, and the En_{Re} of the i^{th} CH is Re^{i}_{CH}, the average En_{Re} of the i^{th} cluster is Re^{i}_{Cl}, and the number of SUs in a cluster is M_{tot}, so the average En_{Re} of the network is computed as follows:

$$Re_{Net} = \frac{\sum_{i=1}^{k} Re^{i}_{Cl}}{\sum_{i=1}^{M} M_{tot}} \tag{24}$$

Also, the average En_{Re} of the CH is determined as:

$$Re_{CH} = \frac{\sum_{i=1}^{k} Re^{i}_{CH}}{K} \tag{25}$$

The FC re-computes the average En_{Re} of the network while it accepts the collective information from CH. If the CH energy level is lower than the average En_{Re} of all the SUs, FC sends overall re-clustering information forces to the entire network accomplish re-clustering.

3 Simulation Results and Performance Analysis

The proposed scheme has been implemented in MATLAB. The prime aim of the simulation was to enhance energy efficiency in the CSS. 100 SUs were randomly deployed in $200m \times 200m$ area of concern. The communication range is 20 m**.** The Distributed Dynamic Load Balanced Clustering scheme analysed the efficiency of the cluster in terms of stability and instability duration, optimal number of CH selection and network lifetime. The proposed DDLBC scheme also evaluated the number of collective information sent to the FC. The performance of the DDLBC scheme was evaluated and compare with the DEEC [6] and ECS [9] schemes in terms of stability and instability duration, optimal number of CH selection, network lifetime, and the number of collective information sent to the FC and also to EESA-RLC [2] in terms of average energy consumption for clusters. The simulation results were studied by varying the network size from 10 to 100. We have incorporated the re-clustering approach jointly with clustering based CSS systems to reduce the energy consumption and also cluster overhead. The aim of comparing clustering performance with associated approaches, we have formulated a Distributed Dynamic Load Balanced Clustering in terms of cluster-based CSS in CR ad hoc networks. The simulation parameters are described in Table 1.

4.1 Bit error rate (BER)

Fig. 3 shows the bit error rate for number of SUs in a cluster versus the average SNR value can be determined from the simulation. The bit error rate (BER) is the number of bit errors per unit time. As the number of SUs increase, the BER decreases with the same SNR. This is because analyse the two different fusion strategies in a cluster to achieve the selection diversity.

4.2 Stability and instability duration

Stability period is the duration of CR ad hoc network performance from the commencing of its operation and first node died out. We compared our DDLBC with the ECS and DEEC schemes proposed in [6, 9]. Fig. 4 shows the total rounds against the number of dead CR ad hoc nodes. As shown in Fig. 4, our DDLBC scheme has higher stability duration than the other schemes. Under DDLBC scheme, the first dead node occurs nearly round 2100, where as the first dead node occur nearly rounds 1600, 1300 under the ECS, DEEC approach. The stability duration of DDLBC compared with ECS scheme increases form round 1600 to round 2100 and the DEEC increases from round 1300

to round 2100. So, DDLBC provides better stability duration (i.e. higher) to prolong the network lifetime than the other schemes.

Table. 1 Simulation Parameters

Network size	**200m×200m**
Communication range	20 m
Initial Energy	1250 mJ
P_d	0.1
Collective information energy cost	50 pj/bit J
Loss factor	0.9
Number of PUs	4
Number of SUs	100
Number of licenced communication channels	4
Packet size	256 bit
CE_T	50nJ/bit
CE_R	50nJ/bit
Number of rounds	5000

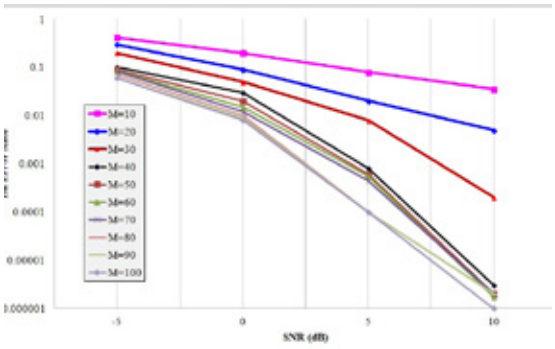

Fig. 3. Bit error rate vs. SNR

Instability duration is the duration between the first dead node and the last dead node within a cluster. Our DDLBC provides lower the instability duration than the other schemes. As shown in Fig. 5, the first node died nearly round 2100 and the last node died nearly 4800. But other ECS scheme provides the first and last node died out nearly 1600, 4200 and DEEC provides 1300, 3100 respectively. Furthermore, the performance analysis concludes that stability duration of DDLBC is better than the ECE and DEEC and also the instability duration is much lower than the ECE and DEEC. This is due to some introduction of gateway user (or intermediate user) to DDLBC, which acts as bridge between the CH and the MN, thus lowering the instability region.

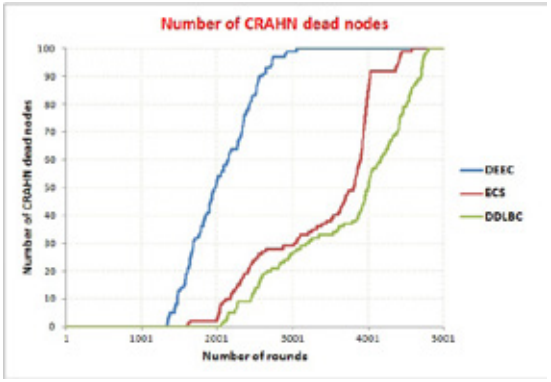

Fig.4. Number of rounds vs. number of CRAHN dead nodes

4.3 Network lifetime

In cluster-based CSS system, network lifetime is the duration of the last alive node in a network. Initially, all nodes are alive in a network. As shown in Fig. 5, out of 100 alive nodes, the first node in the DDLBC scheme died around 2100 and later, nodes died at a regular interval. The ECS and DEEC schemes, there was a rapid increases in dead nodes after the round 1600, 1500 respectively. Fig. 5 shows that our proposed DDLBC scheme provides the reliability of nodes and to prolong the network lifetime. In this approach, the last alive node can still provide the response to the network.

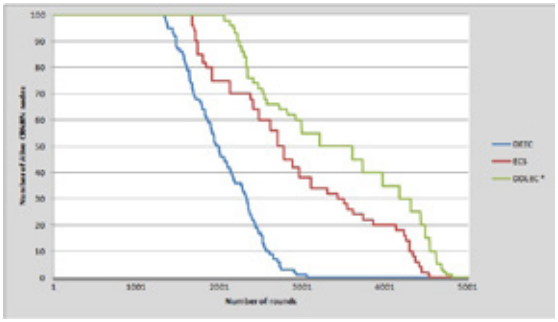

Fig. 5. Number of round vs. number of Alive CRAHN nodes

4.4 Optimal number of cluster selection

From (22), we compute 4 optimal clusters that provide better coverage by increasing the number of MNs or maximising the cluster size in a cluster. It can also reduce the large amount of intra-cluster communication, mostly during transmission. Furthermore, it minimises overlaps between clusters and can reduce the channel conflict between clusters. As shown in

Fig. 6, we compare the clusters with varying the number of SUs in network. Our proposed approach creates fewer clusters to reduce the distance for inter and intra cluster communication. Moreover, not only consider the success of CSS, also consider the network energy consumption when selecting the number of optimal clusters.

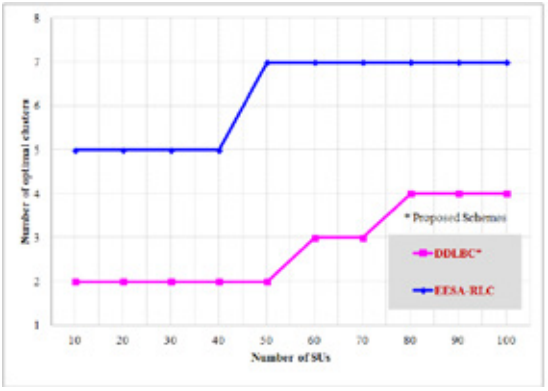

Fig. 6. Number of SUs vs. Number of optimal clusters

From Fig. 7, we can study the result of optimal cluster size in CR network for reducing energy consumption. Energy consumption can be determined from SUs and their own CH for dissimilar clusters. In simulation, we can use 100 SUs to create 4 optimum numbers of clusters to reduce the intra-cluster distances and also reduce the communication between SUs and their CH. This is achieved to reduce the energy consumption in network because of inadequate intra-cluster communication. In a network, for more number of clusters created to reduce the energy consumption of network but inter cluster consumes more energy. So, significantly reduce the energy consumption by calculating the optimal clusters that counterbalance the energy consumption for inter and intra cluster communications. Our proposed DDLBC scheme is minimised the energy consumption and to compute the total number of optimal cluster is four. This is achieved because of balancing among members in each cluster.

4.6 Number of cluster head selection

Fig. 8 indicates the CH selected each round. As shown in Fig. 8, DEEC and ECS schemes resulted in more uncertainty issues for selecting CHs. Under DEEC, random numbers of CHs are selected every round. More CHs are selected under ECS scheme to lead the increase of transmission and sensing cost. Our proposed DDLBC scheme allows CH selection based on energy efficiency which results in low uncertainty. This is achieved because nodes with En_{Re} participate to select the CH. Further, number of CH is selected for each round in a controlled way to extend the network lifetime.

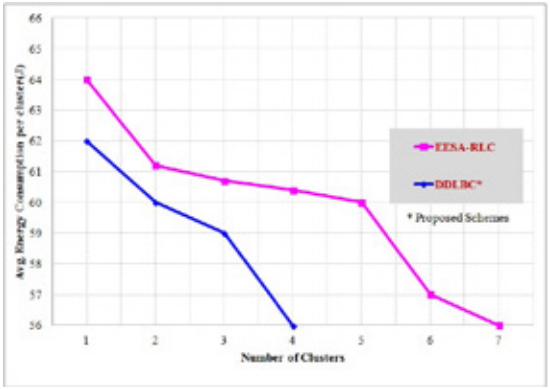

Fig. 7. Average energy consumption for clusters

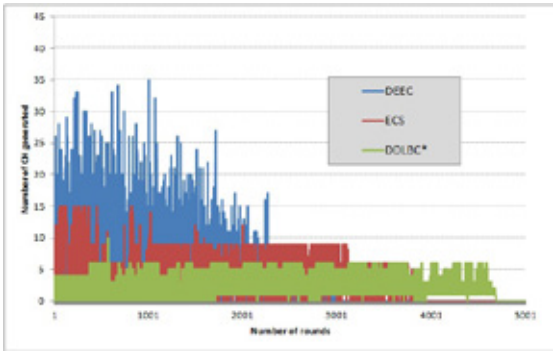

Fig. 8. Optimal number of clusters selection

4.7 Collective information sent to the FC

Fig. 9 shows the collective information send to the FC. Each CH collects the local sensing information from MNs and consolidated into collective information. This is because, if the MNs have enough En_{Re} level to send local sensing information to CH. As shown in Fig. 9, our proposed approach compare with DEEC and ECS. Thus, there is significantly less collective information send to the FC under our proposed approach. This is achieved to prolong the lifetime of network and increase a stability of the clusters under the proposed DDLBC scheme.

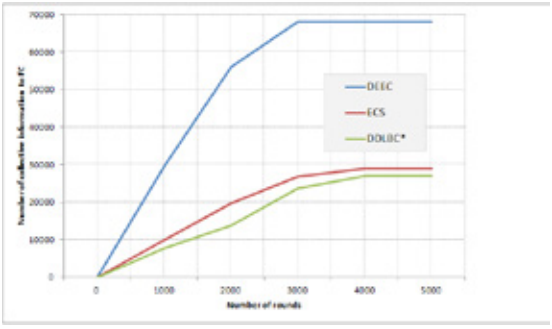

Fig. 9. Collective information sent to the FC

5. Conclusion

We have employed a Distributed Dynamic Load Balanced Clustering scheme to reveal the grouping of MNs into some clusters to minimize energy consumption and increase the sensing capability in CR ad hoc networks. Our prime aim is to enhance the energy efficiency of CSS based on clustering scheme. In addition, the sensing accuracy, network lifetime and cluster stability can also be improved. We used dynamic clustering scheme to select an optimal number of clusters as well as CHs. A node with enough initial and residual energy only can participate for selecting the CH to reduce the energy consumption. A collection information packet can be transmitted through an idle channel when the CHs select to cooperative gain, avoiding unnecessary channel sensing. This is a novel approach to enhance energy efficiency and encourage efficient cooperation among CHs and MNs. This proposed approach also analysed the energy consumption, network lifetime and stability of the clusters. Simulation results revealed that the proposed DDLBC scheme outperforms than other schemes. This is the first work that uses the Distributed Dynamic Load Balanced Clustering scheme for enhancing energy efficiency and prolongs the network lifetime in CR ad hoc networks. In further, we consider the participation of more PUs and also analyse network convergence and fusion strategies for our proposed DDLBC scheme.

References

1. Federal Communications Commission, Docket No 03-222, Notice of Proposed Rule Making and Order, *Federal Communications Commission*: Washington, DC, USA, 2003.
2. Jayanthiladevi A & Kadharnawaz GM, An Efficient Utilization of Spectrum in Seamless Mobility by using Retransmission Rerouting Mechanism in Mobile IP, J of Sci & Ind Rsrch, 74(09) 2015.
3. Lo, B.F, Akyildiz, I.F. *Reinforcement learning for cooperative sensing gain in cognitive radio ad hoc networks*. *Wirel. Netw.* 2013, *19*, 1237–1250.
4. IF Akildiz, Be Lo, R Balakrishnan, Cooperative spectrum sensing in cognitive radio networks: A survey, Physical Communication (Elsevier), vol. 4, pp. 40-62, 2011.
5. Akan, O, Karli, O, Ergul, O. *Cognitive radio sensor networks*. *IEEE Netw.* vol. *23*, pp. 34–40, 2009.
6. L. Qing, Q. Zhu, and M. Wang, *Design of a distributed energy-efficient clustering algorithm for heterogeneous wireless sensor networks*, Computer Communications, vol. 29, no. 12, pp. 2230-2237, 2006.
7. G. Smaragdakis, I. Matta, and A. Bestavros, *SEP: a stable election protocol for clustered heterogeneous wireless sensor networks*, Tech. Rep., Boston University Computer Science Department, 2004.
8. Jayanthiladevi A & Kadharnawaz GM, Optimized Retransmission Mechanism to Prevent Wastage of Spectrum in Seamless Mobility Handover, Intl Jnl of Applied Engg Research, 10 (2015) 3906-3910..
9. A. Rauniyar and S Y Shin, *A Novel Energy-Efficient Clustering Based Cooperative Spectrum Sensing for Cognitive Radio Sensor Networks*, Int. Jour. Of Distributed Sensor Networks, 2015.
10. Kok-Lim Alvin Yau, Nordin Ramli, Wahidah Hashim, Hafizal Mohamad, *Clustering algorithms for Cognitive Radio networks: A survey*, Elsevier. Jour. Of Network and Computer Applications, vol. 45, pp. 79-95, 2014.
11. W Zhang, Y Yang and CK Yeo, *Cluster-Based Cooperative Spectrum Sensing Assignment Strategy for Heterogeneous Cognitive Radio Network*, IEEE Trans. On Vehic. Tech, vol. 64, no. 6, pp. 2637-2647, 2015.
12. Zhang, H., Zhang, Z., Dai, H., Yin, R., & Chen X, *Distributed spectrum-aware clustering in cognitive radio sensor networks*. In GLOBECOM - IEEE Global Telecommunications Conference. [6134296] 10.1109/GLOCOM.2011.6134296, 2001.
13. Md. Sipon Miah, Heejung Yu, Tapan Kumar Godder, and Md. Mahbubur Rahman, *A Cluster-Based Cooperative Spectrum Sensing in Cognitive Radio Network Using Eigenvalue Detection Technique with Superposition Approach*, Inter. Jour. of Distributed Sensor Networks, 2015.
14. Ben Ghorbel, M.; Haewoon Nam; Alouini, M.-S., *Cluster-based spectrum sensing for cognitive radios with imperfect channel to cluster-head*, in Wireless Comm. and Networking Conference (WCNC), pp.709-713, 2012.

15. Chunhua Sun; Wei Zhang; Ben, K., *Cluster-Based Cooperative Spectrum Sensing in Cognitive Radio Systems*, IEEE Inter. Conf. on Communications, ICC '07, pp.2511-2515, 2007.
16. Jayanthiladevi A & Kadharnawaz GM, *"Analysis study of Seamless Integration and Intelligent Solution in any situation by the Future Advanced Mobile Universal Systems 4G -(FAMOUS 4G)"*.
17. Zhiquan Bai; Li Wang; Haixia Zhang; Kyungsup Kwak, Cluster-based cooperative spectrum sensing for cognitive radio under bandwidth constraints, IEEE Inter. Conf. on Comm. Systems (ICCS), pp.569-573, 2010
18. Nhan Nguyen -Thanh and Insoo Koo, *A cluster-based selective cooperative spectrum sensing scheme in cognitive radio*, EURASIP Journal on Wireless Communications and Networking, 2013.
19. Ying Wang, Yan Huang, Wenxuan Lin and Weiheng Ni, *Optimization of Cluster-Based Cooperative Spectrum Sensing Scheme in Cognitive Radio Networks with Soft Data Fusion*, Journal Wireless Personal Communications, vol. 77, no. 4, pp. 2871-2888, 2014 .
20. Jianzhao Zhang, Fuqiang Yao, Hangsheng Zhao, *Distributed Clustering in Cognitive Radio Ad Hoc Networks Using Soft-Constraint Affinity Propagation*, Radioengineering, vol. 21, no. 3, pp. 785-794, 2012.
21. T Kumar, R Muthukkumar and N Shanthi, *Review of Mobility Aware Clustering Scheme in Mobile Adhoc Network*, IJCA Proceedings on International Conference on Research Trends in Computer Technologies 2013 ICRTCT(1):19- 24, February 2013.

This page was left blank intentionally!

The Bauhaus movement and its influence in graphic design, visual communication and architecture in Greece

Konstantinos Kyriakopoulos

Hellenic open university,Faculty of applied arts graphic arts & multimedia, Greece
E-mail: calavria@acci.gr

Summary

This paper attempts to present the elements defining the philosophical approach, the characteristics and the style of the Bauhaus movement. More specific it presents the social background of the period during which this school was established and the vision of its main representatives. It analyzes the way it influenced graphic design, visual communication and architecture in Greece. A comparison has been made between typical Bauhaus works and works of contemporary graphics aiming to find how they were influenced by the Bauhaus movement.

Especially, it presents the projects (posters and buildings) and the artists who worked according to the Bauhaus rules. This is a small research of how the Bauhaus school influenced modern graphic art and visual communication design in Greece until today.

The conclusion of this research is that the Bauhaus movement which was the first to combine art with technology to obtain clarity and functionality rather than aesthetics, still has a crucial affect on modern design, graphic arts and visual communication in Greece.

Chapter 1: The second half of the 20th century

Bauhaus's influence is obvious in many countries in the world, including Greece. The Architect Ioannis Despotopoulos (1903–1992) was the only Greek student who studied at the Bauhaus School. However, a lot of Greek designers embraced the Bauhaus movement and followed it's ideas in visual communication. From the 1950 this influence can be found in many Greek designer's projects, such as in the creations of G. Vakirtzis, M. Katzourakis etc., mainly on posters designed for the Greek Tourism Organization. Later, Greeks who studied abroad, followed the Bauhaus design principles and created projects with the same characteristics, as for example the projects of D. Arvanitis, V. Karatzas and J. Kouroudis.

This influence of the Bauhaus movement in graphic arts in Greece which is obvious from the mid-20th century, postwar, is first seen in a structured production of posters made in 1946. The GNTO (Greek National Tourism Organization) assigns the poster series creation to the artists Spyros Vassiliou, Panagiotis Tetsis, Yannis Moralis **(Figure 1)**, Pericles Byzantios and Lambros Orfanos to be followed by the younger generation with George Vakirtzis with movie posters, Dimitris Mytaras Michael Katzourakis, Freddie Carabott, George Anemogiannis (Rapidis, ch.i.). with printing works of Bauhaus, clearly influenced by the Swiss School **(Figure 2)**.

Figure 1: Tourist poster: Hydra Yannis Moralis, Athens, 1956,Greek National Tourism Organization

Figure 2Tourist poster, painting of Kastella George Vakirtzis, Piraeus, 1955, Teriant Museum.

George Vakirtzis specialized in engraving and graphic arts at École des Beaux-Arts in Paris (1923-1940). As an artist he worked with several advertising companies. He was the Greek version of the poster's forefather Henri Toulouse Lautrec. Their similarities are plenty. Both talented painters, they did not accept all the graphic styles but instead focused on designing posters for the promotion and communication of shows. Vakirtzis' parallel work with product promoting posters, constitutes an extension of his main job of film promotion (Margaritis, ch.i). His Expressionistic, anthropocentric imaging technique was representational but with all the features of the Swiss style and with bold, vibrant colors. This contemporary, capturing way of imaging raised this contemned kind of art to a new and unique artistic and ideological level.

In his other works, Vakirtzis seems to follow the Bauhaus principles more staunchly (MMCA).

Michael Katzourakis', Freddie Carabott's and Agne Katzourakis' posters logos and ads based on Envan image modernism, imposed a new promotional language, fresh, minimalistic and at the same time very Greek. As direct references the sidelong glances at antiquity, Byzantine tradition and folk art, interspersed with a good sense of humor, they created a globally recognizable picture of Hellenism and became the deacons of a charming, modern "Greek style" (*Rigopoulos, 2007*).

Michael Katzourakis, studied at the school of Paul Collin in Paris in the early 50s and was one of the most important graphic designers in postwar Greece, having obtained great excellence -together with Freddie Carabott, who had studied graphic design in London, first at Chelsea and then at St. Martin School Of Art - during hard decades for the visual communication in Greece (*Diamantopoulos, 2011*).

The geometric abstraction played a leading role in his art work, which is why Harry Savvopoulos referred to Michael Katzourakis as one of the pioneers of Greek geometric art. A review written about the exhibition held in Denise René gallery in Paris 1999, the following review was written: "Simplicity, economy of means, limited expressiveness, sensitivity, pulse, organic autonomy and architecture, monumentary perception of form" are some of the features of the visual artist Michael Katzourakis (*Diamantopoulos, 2011*).

What Katzourakis was aiming in the poster design was "to escape from the detailed illustration and instead obtain a significant visual function through the connection of a simple and clear visual style and a clear message." Michael Katzourakis and Freddie Carabott was those who brought the "idea" to Greek advertising, the famous concept (*Rigopoulos, 2007*).

D. Fatouros had argued, with some exaggeration, that the Greek simplicity in some foreign posters is striking, the use of symbols and forms, with an impressive use of Tsichichold's rules with vertical and lateral text formatting, exclusive san serif fonts, the use of spaces, etc. well known features from Vakirtzis' three Greek posters from the exhibition and the post-war period. The espousal of Bauhaus principles, aimed to a better way to spread the message through the clear printing.

Freddy Carabott and Michael Katzourakis appear in the field of visual communication at the end of the fifties, when the design has been transformed from an empiric situation to a full developed new art form. Posters, logos and entries had completely changed the setting. They imposed a new promotional language: minimalistic, influenced by the spirit of Bauhaus, fresh, yet authentically Greek, with frequent indirect references to antiquity, the Byzantine tradition and folk art, with an attractive, contemporary Greek style **(Figures 3-4)** aiming to achieve a fast transmission of the visual message and a clear choice of words.

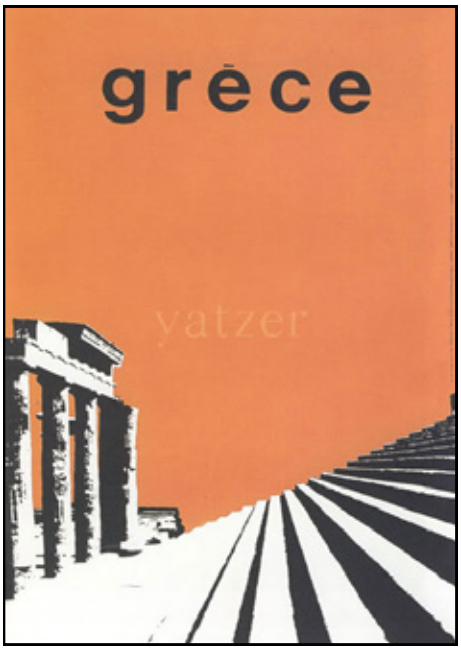

Figure 3: Freddie Carabott, 1963, Poster for GNT

Figure 4: Katzourakis Michael, 1965, Poster for the Epidaurus Festival

The influence of Bauhaus is evident in all their works, mainly minimalism and clean fonts. In Michael Katzourakis, pioneer and founder of the Greek style, early works, the thematic start point derives from the world of everyday objects. His research steers him to the promotion of fundamental geometric elements, in the way they emerge from the correlations of the horizontal and vertical line and the interaction of the color relations to strong contrast. The use of a single photo and the simplification of material comes from the corresponding posters of Swiss Tourism (MMCA).

Michael Katzourakis had mentioned- in an interview to Thanassis Diamantopoulos (2/3/2011) concerning his team's work on tourism and tourist posters- that they worked as art consultants for the Greek Tourism Organization from 1959 -1967, with the agreement that they would have full freedom to work for new, fresh creations. The team worked the traditional way: Photographing objects, photo montage and paintings. They tried hard to get the equipment and all what was necessary for their work, which did not exist in Greece then.

Especially when the Helvetica font came in Greek, Katzourakis as a real student of the Swiss school, says that they used it, photographed it from the manuals, cut the letters one by one and glued them back together one by one again. This is a direct admission to the Bauhaus print design (*Diamantopoulos, 2011*).

Chapter 2: The last decade of the 20th century – 21st century

Dimitris Arvanitis studied painting and graphic arts in Belgium and is currently the main representative of the Swiss school in Greece. Since 1973 he works designing CD covers, books, posters and no advertising programs at all. The poster of road safety **(figure 5)** is a clear example of the influence of the Swiss school, the bright red color and simplified picture that fills up the surface in a "threatening" way. Arvanitis has designed dozens of Jazz posters **(figure 6)** in which the vertical and horizontal text formatting are dominant pointing to the 20s of Bauhaus Weimar (*Nenes, G. 2012*).

Figure 5: Dimitris Arvanitis, 2011, poster for road safety.

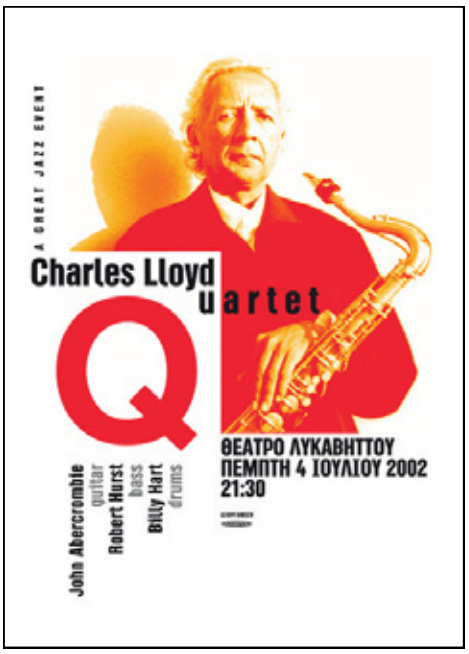

Figure 6: Dimitris Arvanitis, 2011, exhibition poster in Heraklion on the Jazz.

The Bauhaus influence in graphic design in our country is more than clear. The front pages designed by Dimitris Arvanitis for the Graphic Design and Communication magazine IFFEN **(figure 7)**, are defined by the purity and minimalism of Bauhaus, as well as the powerful contrasts of the Swiss School.

In the book covers designed by Arvanitis, as for the magazine **(Figure 8)** "Routes", the vertical and slanted text formatting are used, a style in straight line with Bauhaus principles, the excessive removal of white spaces and the leading - exclusive role of the fonts comes directly from the posters of Herbert Beyer, which also appears in the "Agenda" cover 2009 with the title **"**where do dreams go when you wake up?**" (image 9)**, with powerful compositions on horizontal and vertical text formatting and the clarity provided by the placard setting.

Figure 7: Dimitris Arvanitis, IFFEN cover of the magazine.

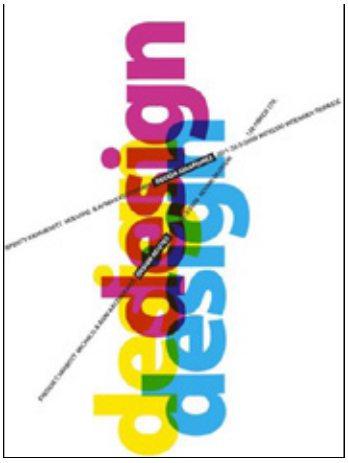

Figure 8: Dimitris Arvanitis, Cover for the Design book tracks, 2008.

Figure 9: Dimitris Arvanitis, Cover for Agenda 2009, Scooter Books, 2008, Athens.

Young artists of the 90s, like Vangelis Karatzas who studied in England, form the design of magazines based on asymmetrical paging and Bauhaus principles. With Vangelis Karatzas, as the art director, the "Status" magazine **(Figure 10)** following the same design rules, with asymmetric text arrangement and form clarity, offers an excellent design result focusing on the visual and verbal message through minimalism. The article is now considered as a set of texts and pictures placed in a rectangle, while the rejection of the center oriented text formatting, as seen in the layout of the magazine "Pictures of the World" **(figure 11)**, texts and images of of the classical typographic settlement, offers unlimited composition possibilities compared to the static classical form.

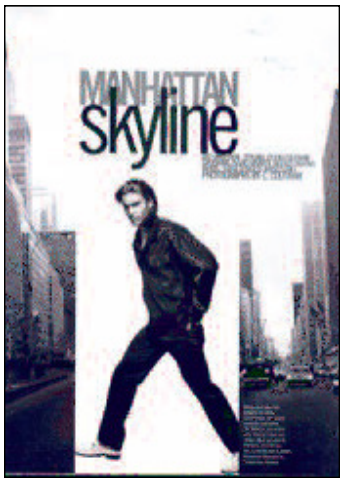

Fig.10: B. Karatzas, magazine page Status, 1996.

Figure 11: V. Karatzas, magazine page Pictures of the world, 1997.

The 16th Graphic event organized in Istanbul on April 27 an online poster competition for the World Graphic Design Day ICOGRADA, with the title "Kalimera Mellon / Merhaba Gelecek / Good Morning Future". The poster released **(Figure 12)** is designed at 72 dpi, in jpeg format and RGB color model (Greek Graphic Designers Association, ch.i.). This constitutes a clear reference to the cover of the Bauhaus catalogue STAATLICHES BAUHAUS IN VEIMAR 1919-1923 designed by Herbert Bayer. The catalytic influence of Bauhaus is easily perceived. Placard background, expressive, powerful clarity and printing, the using of fonts without serif for instant, effortless communication.

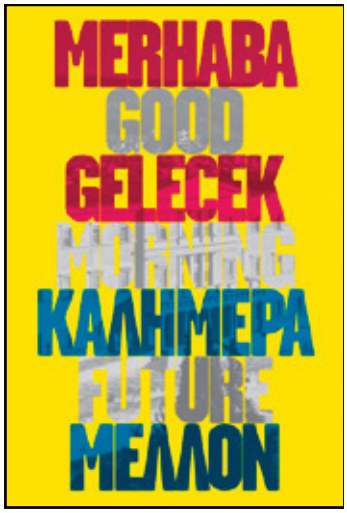

Figure 12 Online Poster Design: 1024 * 768 pixels 72 dpi, to "climb" the official site of Grafist16.

Modern posters with cultural content was designed based on the principles of Bauhaus, that is by the use of photo printing (phototypography), the diagonal lines, geometric shapes and placard backgrounds, as the poster **(picture 13)** released by the Community Centre "Melina Mercouri", Ilion municipality. According to the Bauhaus spirit was also the released poster for the Photo Festival in Old Arsakeio, in Patras **(picture 14)** of which the characteristic features was the diagonal arrangement of the text asymmetry synthesis and minimalism which point to the school of Bauhaus. The poster used by Konstantinos Andronis for his Photo Exhibition **(Figure 15)**, is largely imitating the Bauhaus technique, where the text forms a picture, while the whole of that image and photography forms the final image.

Pictures 13-14-15 : Posters with cultural content. Photography Festival Arsakeio School of Patras, 2012

Greek Universities are adopting the Bauhaus design principles in the layout of their guides. The school's influence and impact on nearly all art schools around the world is apparent. It's also observed in Greece **(Figure 16)**. The Study Guide cover of the Faculty of Fine Arts in Athens University refers to asymmetric printing of Jan Tscichold on the cover of the magazine *Elementary Typography* in 1925.

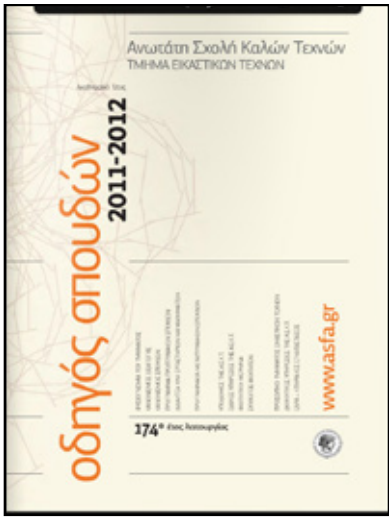

Figure 16: The cover Study Guide of the Faculty of Fine Arts in Athens University, 2012

The education and practice methods which are known as basics or as Bauhaus methods became the basis of all art teaching. This form is observed the same side layout of the text, as respectively happens in Bauhaus, while dominated by simple colors, the layout of text and placement of linear elements in italic fonts and clean geometric shapes which strengthen the minimalist spirit of design. (*Tsioutis, 2010: 66,67*).

Chapter 3: In the 21st century – now days

The new word, in terms of design and visual communication, does not mean that it has never existed before. This limitation set by clients, markets, technological requirements, is always formed in a way that the public can easily understand it. But for those who want to create a completely new design, the continuous link with the past is a frustrating paradox. Raymond Lowe, the industrial designer who managed to significantly change both the function and the appearance of products and equipment from 1930 to 1960, admitted the existence of this paradox and developed a concept he called "Sophisticated but acceptable."

Figure 17: Kouroudis John, 2000; Packaging for Korres' products.; Minimalist design approach.

For the design of packaging Korre's products **(Figure 17),** there was a design approach of the Bauhaus principles, minimalism and simplicity. That is what the creator, graphic designer J. Kouroudis wants to explain *"if you see the bottle you realize that it is the most common jar on the market and the only difference is the tops. That is the luxury we put on it, the design played a substantial role to differentiate the product from the rest. The minimal and simplicity of this creation took the luxury to simple"*. The aim of this design approach is the emergence of simple, natural element that has no need of any support, until the emergence of the identity as a genuine product of a social good accessible to all (*Memou,*

2001, t.15: 28). The same occurs with the inclusion of dartbooks in the magazine «+Design» **(Figure 18)**, where the colors, the layout of text and placement of linear elements in italic fonts and clean geometric shapes refer to the Bauhaus. Also in the poster designed by D. Arvanitis **(Figure 19)**, in which is clear the influence of Bauhaus design. Clarity, geometric shapes and minimalism are the characteristics in this poster.

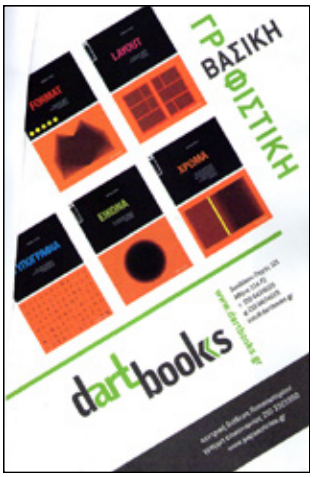

Figure 18: Dart Books: Advertising in Magazine "+ Design" September-October, Athens, 2006

Figure 19: D. Arvanitis, Poster: NO RACISM Panorama Design, 2013

It has now become a tradition in recent years, the logo of the respective Final Four Euro league basketball **(Figures 20, 21)**, to be designed by Greek creators. The baton gets this year the new Greek Semiotik Design Agency, and with a signal having very strongly "design character", having direct reports in one of the most influential schools of the last century design, which although was active in Germany, but the stigma of it is felt even nowadays worldwide.

The new logo, inspired by the Bauhaus, carries the basic features of the movement, such as simplicity and functionality, with particular emphasis on geometric forms and color, discarding any unnecessary embellishment. Direct references are in geometric forms and compositions of works of Joost Schmidt (1893-1948) and Herbert Bayer (1900-1985), and especially in the second draft of the font, Universal Alphabet and the first initial "b".

While having as main theme the ball and the floor plan of a basketball court, a strong signal was generated, showing both the sport, and Berlin itself.

As and Euro league Basketball to the official presentation of "the logo merges the soul of basketball and the city of Berlin, combined in perfect harmony with the movement style of the Bauhaus, which has been a pioneer in setting the ground rules and patterns of modern design ".

"Athens Design" is the rebranded name of the most successful annual communication design conference in Greece. After ten years as a Design Panorama, its organizers decided that it was upon time to breath some fresh air into this respectable institution. *"We were called to help shape the new brand,*

envision an international event, with a Greek suggestion The result of our design process reflects early Greek typographic action.

Figure 20

Figure 21

Figure 20, 21: Logo for the Final Four Euroleague Basketball 2016; Semiotik Design Agency, 2016

Chapter 4: The influence of Bauhaus in greek architectural design

Professor John Despotopoulos (1903-1992) who studied at the School of Bauhaus, was involved in the development of modern architecture in Greece during the '30s. The Cultural Center of Athens is one of the most important projects, and was awarded for the study, of which held only a small part in today's Athens Conservatory (*Petridou, 2009: 12-13*).

Early Bauhaus architecture, however, can be detected in Greece, at the characteristic cubist buildings of Athens, such as the US Embassy -created by Gropius-, which was built with modern techniques, with columns inspired by the Parthenon and Pentelic marble. Also at the War Museum and the National Gallery, in front of the Porto Carras Grand Resort, designed by Gropius, the building of the National Bank in the Republic Square in Thessaloniki and numerous buildings designed by Greek architects who were influenced by modernism and the Bauhaus. Typical examples are the refugee blocks of Alexandras Avenue in Athens **(Figure 12)**, the most important example of folk residence in Greece during the interwar period, the work of K. architects. Laskaris and D. Kyriakou, which according to Professor Dimitris Filippides in his book "Modern Architecture" are designed in style purely German Functionalism (*Petridou, 2009: 12-13*).

Picture 12

Picture 13

Picture 12, 13: The Refugee quarters of Alexandras Avenue, in Athens. Architects: K. Laskaris - D. Kyriakou, 1933, Photo: Konstantinos Kyriakopoulos

Nowadays, while the Bauhaus retains its value, speculation and ignorant governments are destroying many buildings of its kind. The hotels "Xenia" Aris Konstantinidis and other architects did not stand as lucky as the Refugee quarters of Alexandras Avenue, which after a long struggle finally was classified as preservation area(Elliniadis, 2009). Another Bauhaus artwork in Athens worth mentioning is the American Embassy building in Vasilissis Sofias Street **(Figure 13)**, a typical work of the school, built in 1959 by the same Walter Gropius. Also the War Museum of Athens **(Figure 14).**

Picture 13: The American Embassy in Athens, Gropius, 1959.

Picture 14: War Museum of Athens, Architecture: Balentis Thoukididis, 1964

Conclusion

The Bauhaus movement influence on the visual communication designers in Greece had given birth to a stream that resulted in the creation of a series of works based on the principles of this modern style. The Minimalism and functionality of this design trend - using the vertical text formatting, the implementation of the diagonal direction both on linear elements as well as in the text -got through the times and are widely used till today. This is confirmed both by the font designers, and the poster designers, as in the case with the contemporary Frutiger font which at the end is a remake of the Frutiger font from the Bauhaus period. New technologies, through digitization, are used in graphic design without ignoring the Bauhaus principles. Their applications are not limited to fonts, but also in the whole spectrum of visual communication, in color, form and image.

The sociopolitical context of the Bauhaus period defined the new design flow that ought to shake off, whatever was connected with the past and build a more fair society. This trend occupied and influenced all the Greek post-date, applied art schools, graphic design and visual communication in Greece. Putting aside decoration and ornaments many artists created great works based on simplicity and functionality. Consequently, a design arises that favors functionality and clear forms, and this is exactly what John Kouroudis, graphic designer and creator of the packaging of the Korres products, did. He left all unnecessary features aside and kept what was useful focusing on simplicity and functionality. He applied the Bauhaus principles and achieved design optimization.

This movement's influence in graphic design was taken after by a large number of designers who implemented the clear graphic design in word and picture, reflecting the dialogue between Bauhaus and modern graphic design.

Influences of Bauhaus architecture can be also detected in Greece. The US Embassy -created by Gropius-, the War Museum and the National Gallery of Athens, the Porto Carras Grand Resort -designed by Gropius-, the building of the National Bank in Republic Square, in Thessaloniki, and other buildings were designed by Greek architects who were influenced by modernism and Bauhaus. A Typical example is the refugee apartments in Alexandra's Avenue in Athens.

References

Diamantopoulos, Th. (2011, April 2). Michael Katzourakis: The leader of the Greek style. Retrieved April 20, 2012, from http://www.e-go.gr/culture/article.asp?catid=18476&subid=2&pubid=114266686

Diamantopoulos, Th. (2011, October 23). MICHAEL KATZOURAKIS: The patriarch of visual communication. Retrieved April 25, 2013, from

http://www.ethnos.gr/entheta.asp?catid=23310&subid=2&pubid=63475277

Elliniadis, S. (2009 Augustus 9). The trend did revolution. Free press. Retrieved March 12, 2012, from http://www.enet.gr/?i=news.el.article&id=71049.

Kouroudis, C. (2001). The graphic designer is the director of the Graphic Arts. LTD: + Design, vol. 15, Athens: Graphopress, pp 26, 28.

Nenes, C. (2012, March 26). Dimitris Arvanitis. Retrieved May 22, 2012, from http://www.athensvoice.gr/article/culture/art/δημήτρης-αρβανίτης

Tsioutis, N. (2010). Creative waves. LTD: + Design, vol. 68, Athens: Graphopress, pp. 67, 68.

Hoursoglou, K. (2005). Greek Industrial Design. LTD: + Design, vol. 48, Athens: Graphopress, pp. 65, 66.

Websites

Vakirtzis, C. (Ch.i.). Retrieved March 30, 2012, from http://www.thf.gr/default.aspx?lang=el-GR&page=14&mode=3&artist=868

Greek Graphic Designers Association (ch.i.). Retrieved May 25, 2012, from http://gda.gr/content/δρωμενα-grafist-16-online-design-poster.

Margaritis, X., Upcoming. Album posters and designs for the cinema of George Vakirtzis, Retrieved May 22, 2012, from http://gda.gr/content/προσεχώς-λεύκωμα-με-τις-αφίσες-και-τα-σχέδια-για-τον-κινηματογράφο-του-γιώργου-βακιρτζή

Mastoridis, K. (2012). The Graphic Arts in Greece. Example for Cyprus? Retrieved 7 January 2013, from http://unic.academia.edu/klimismastoridis/Papers.

Macedonian Museum of Contemporary Art. Retrieved May 22, 2012, from http://www.mmca.org.gr/mmst/el/collection.htm?m=1&l=10;419:bio

Petridou, K. (2009, December 15). Bauhaus-Bauhaus: 90 years to close the School changed data. Tee, vol. 387, pp. 12-13. Retrieved February 8, 2012, from http://portal.tee.gr/portal/page/portal/teetkm/GRAFEIO_TYPOY/TEXNOGRAFHMA_2009/TEXNOGRAGHMA_387/387%2012_13.pdf.

Rigopoulos, D. (2007, December 7). The Greek style was born in '60. Retrieved April 25, 2013, from http://news.kathimerini.gr/4dcgi/_w_articles_civ_0_04/11/2007_247269